Depositional environment and sequence stratigraphy of siliciclastic - carbonate deposits of Parvadeh Formation (Middle Jurassic) in Tabas block, East Central of Iran

Vesal Yahya Sheibani[1], Reza Moussavi-Harami[2], Asadollah Mahboubi[2]*, Mohammad Khanehbad[2]

[1] *Department of Geology, Faculty of Science, Ferdowsi University of Mashhad, International Campus, Iran*

[2] *Department of Geology, Faculty of Science, Ferdowsi University of Mashhad, Iran*

**Corresponding author, e–mail: mahboubi@um.ac.ir*

(*received: 27/08/2019 ; accepted: 20/01/2020*)

Abstract

Parvadeh Formation (Bathonian) in Tabas block is formed of mixed siliciclastic-carbonate deposits. Six stratigraphic sections have been selected in this formation which dominantly composed of conglomerate, sandstone, shale and limestone. Integration of field and microscopic studies resulted in identifying two facies association including 4 siliciclastic and 10 carbonate facies in this formation. Analyzing facies and sea level fluctuations caused identification of two 3rd order sedimentary sequences in each of the sections. The low-stand system tracts of the recorded sequences are characterized by tidal flat and lagoon facies and shallowing-upward para-sequences. Highstand and transgressive systems tracts are generally both represented by dominantly intertidal and sub-tidal lagoon, shoal and open marine facies. The upper and lower boundaries in all stratigraphic sections of middle Jurassic successions are SB1 that are distinguished by erosional evidences and sometime red conglomerate and sandstone horizons. On the basis of detailed facies and depositional sequences analysis, global sea level fluctuations and tectonic events are the most important factors that affected system tracts and depositional sequences in the Tabas block. Local tectonic activities (mostly related to Kalmard and Nayband Faults) also have an effective role on the thicknesses of siliciclastic and carbonate deposits in different parts of study areas.

Keywords: *Parvadeh Formation, Middle Jurassic, Sedimentary Environment, Microfacies, Sequence Stratigraphy.*

Introduction

Jurassic deposits in central Iran, and particularly in the Tabas block, are highly developed and have been studied by numerous researchers (Aghanabati, 1975; Seyed-Emami *et al.,* 2000; Fürsich *et al.,* 2003; Wilmsen *et al.,* 2003; Wilmsen *et al.,* 2005; Wilmsen *et al.,* 2009a; Wilmsen *et al.,* 2010; Zamani-Pedram, 2011; Salehi *et al.,* 2017). Parvadeh Formation as the first Formation of Magu Group of Central Iran deposited after Middle Cimmerian event and its type section was measured and introduced by Aghanbati (2006), on the western slope of Eshelon Mountain and extensive studies have been done on it by Iranian and other foreign geologists, including Seyed-Emami *et al.,* (2004), Mehdizadeh (2010), Rahmani (2014a), Rahmani *et al.,* (2014b), Rahmani *et al.,* (2014c) , Valipour Gudarzi *et al.,* (2015), Zarrin *et al.,* (2016), Pandey & Fürsich, (2003) & Seyed-Emami *et al.,* (2004). Tabas block has been affected by the sea level fluctuation and many tectonic activities in global, regional and local scale, especially at the time of middle and late Jurassic led to formation several sedimentary basins with various lithofacies (Seyed-Emami *et al.,* 2006; Wilmsen *et al.,* 2009a). After the ending sedimentation of Middle Cimmerian event, Parvadeh Formation was deposited. Type section of this formation with 46 m thickness was measured and introduced in the western part of Eshelon Mountain (Northwest of Tabas) (Aghanabati, 1998, 2006). This formation outcropped in different parts of sedimentary structural zones of Tabas block such as Shirgesht, Kalmard, Abdoughi, and Ravar and this rock unit is located as a key bed between Hojedk sandstones (below) and Baghamshah marls (above). In this paper, six stratigraphic sections, of the Parvadeh Formation were selected to describe facies and characterize detailed sequence of stratigraphic framework of the mixed carbonate-siliciclastic deposits. These sections were selected according to the Aghanabati's divisions for Iran's sedimentary-structural zones (2006), and included Kal-e-Shur, Mazino, Chah-e-Kamardoshakh (Abbas Abad), south of Parvadeh, Sikhuri and Kalshaneh, in various sub-blocks of Tabas block. Mixed carbonate-siliciclastic successions have been described in many Phanerozoic sedimentary basins which were affected by various factors including tectonics, eustasy, climate, in situ carbonate production and variations in siliciclastic sediment supply (Tucker, 2003; Tcherepanov *et al.,* 2008; Catuneanu *et al.,* 2011).

Geological Setting

The study area is located in Tabas block as a part of Central-East Iranian Micro-continent (CEIM). It became detached from Gondwana during the (Late) Permian and collided with Eurasia (Turan Plate) in the late Middle – early Late Triassic, there by closing the Palaeotethys (e.g. Berberian & King 1981; Boulin, 1988; Alavi *et al.,* 1997; Saidi *et al.,* 1997; Stampfli & Borel 2002). The CEIM consists of three north–south oriented structural units, called the Lut, Tabas and Yazd blocks, which are today aligned from east to west, respectively. Tabas block is a part of the vast territory of central Iran with a very complex geologic and structural history which is the most complex and disturbed geological unit of Iran. In fact, this zone can be considered a collection of different suspect terrains that have been linked together during long geological times and different geotectonic activities and movements (Nazemi, 2013). The Tabas fusiform block is separated from the Posht-e-Badam and Yazd blocks by the Nayband fault (from the east) and the Kalmard-Kuhbanan fault (from the west). The mentioned large north-south direction faults have been formed since the beginning of the structural evolution of central Iran and have been divided into different facies and sedimentary basins since the Infracambrian (Stocklin, 1968; Berberian & king, 1981).

Parvadeh Formation has a very good outcrop in Tabas block and many of its properties such as bedding and skeletal and non-skeletal components are clearly observable in the field. These sections are respectively located at 130, 91, 95, 83, 63, and 85 km of Tabas city. On the basis of previous studies, the age of this formation is Bathonian (Aghanabati, 2006). Kalshaneh and Kal-e-Shur sections (Tal Hamid), respectively with 46.95m and 54.4m thickness, are located in Kalmard block; Mazino and Chah-e-Kamardoshakh (Abbas Abad), respectively with 58.85 m and 54.33 m thickness, are located in Ravar-Mazino sub-block; and South of Parvadeh section, with 79.64 m thickness is located in Nayband sub-block; and Sikhuri section, with 49 m thickness is located in Shotori block (Fig. 1). The lithology of this formation consists of conglomerate, sandstone, ooidal-oncoidal, and fossiliferous (including coral, bivalve, brachiopods, echinoderm, ammonite, sponge, and bryozoan) limestone, shale and mudrocks. This formation almost in all sections is situated with an erosional surface on Hojedk Formation and is situated conformably below Baghamshah Formation.

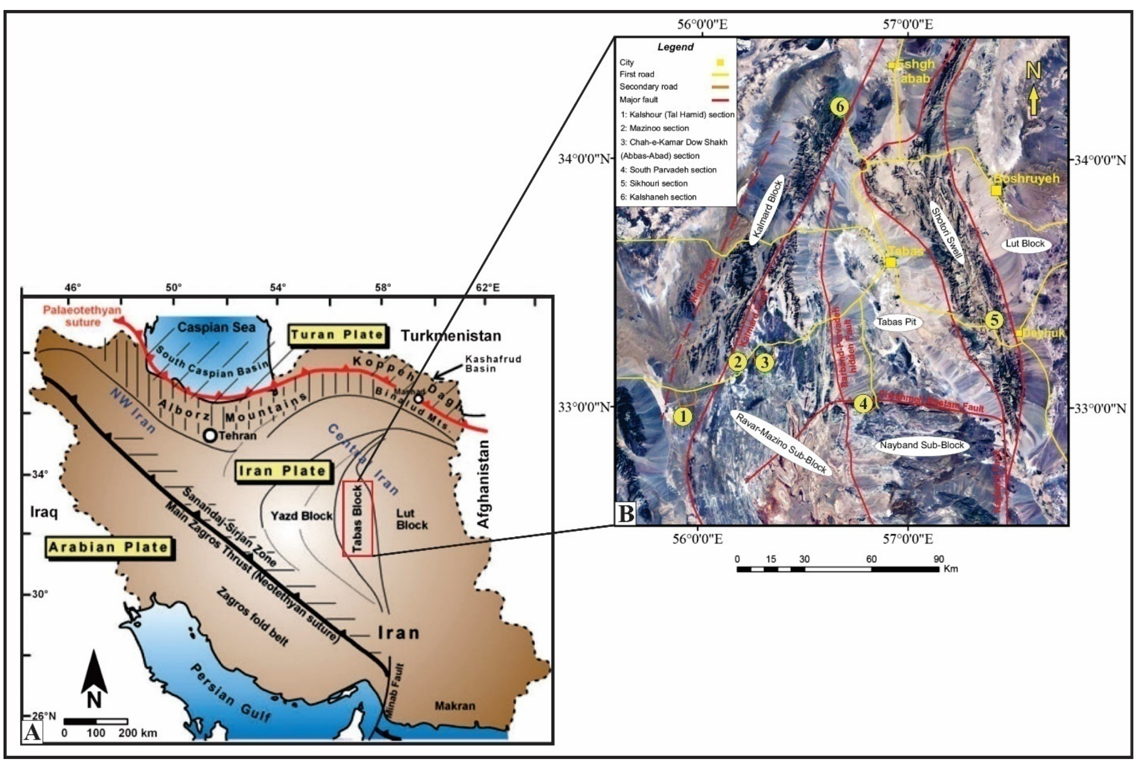

Figure 1. Structural zones of Iran (A) (Wilmsen *et al.,* 2009a) and location map of studied sections (B), No.1: Kal-e-Shur section, No.2: Mazino section, No.3: Chah-e-Kamardoshakh (Abbas Abad) section, No.4: South of Parvadeh section, No.5: Sikhuri section, No.6: Kalshaneh section.

In Sikhuri section, Parvadeh Formation deposits are situated with angular unconformity on the limestones and dolomites of Jamal Formation (Permian). Parvadeh Formation carbonate rocks mainly include fine grain (calcilutite) to coarse-grained (calcarenite) with a variety of skeletal and non-skeletal components that mostly consist of coral, bivalve, brachiopod, echinoderm, gastropod, foraminifera (Fig. 2).

Material and Methods

Six complete sections were selected at the well-developed middle Jurassic succession. A variety of data sets were utilized such as lithofacies, physical sedimentary structures and bioturbation intensity to construct a detailed sequence stratigraphic framework for these deposits. Four hundred and fifty samples were obtained and detailed petrographic examination of thin sections allowed the determination of various microfacies. Siliciclastic and carbonate facies were described following the classification of Dunham (1962) and Folk (1980) classification scheme with the modifications of Embry and Klovan (1972). Identification and Separation of facies were done using ramp facies model of Flügel (2010). Clasticity indices of ooid, intraclast and echinoderm fragments in some facies were measured based on Carozzi (1993). Identification and separation of depositional sequences and facies association, were carried out following Carozzi (1993), Van Wagoner *et al.,* (1988, 1990), Schlager (2003), Catuneanu *et al.,* (2009, 2011, 2013). For better simulation of the sedimentary basin at the middle Jurassic time, depositional sequences, system tracts and sequence boundaries were correlated in all stratigraphic sections. Since no accurate detail study has been done on sedimentology of Parvadeh Formation in the studied area, the aim of this study is the facies description, depositional environment analysis and characterized sequence stratigraphy in these sections.

Facies analysis and depositional environments

Based on a variety of characteristics in Parvadeh Formation deposits such as dominant texture, sedimentary structures, grain size, grain type (skeletal and non-skeletal) and matrix, two main facies associations were identified within these successions. Siliciclastic facies association (T1-T4) included coarse-grained (conglomerate), medium-grained (sandstone) and fine-grained (shale and mud rock). Carbonate facies association (L-O) composed of lagoon, shoal and open marine facies. A detailed description and interpretation of these facies has been mentioned as below:

Siliciclastic facies association (T1-T4)

Four facies were identified in this facies association which had been mostly formed in tidal flat environment and consisted of conglomerate, shale, sandstone, and mud rock facies (Fig. 3).

Subfacies T1: Conglomerate. This lithofacies is usually present at the base of some cycles (fining upward cycles) in the lower part of succession of Parvadeh Formation (Fig. 3A). Conglomerates with different thickness are often in lensed form and bounded at their base by erosional surfaces Sedimentary structures, such as cross-bedding, can be observed in this lithofacies. Conglomerate based on their matrix amounts are ortho- conglomerate (in Abbas Abad, south of Parvadeh and Mazino sections) and para-conglomerate (mostly in Kalshaneh section) and considering the pebble types are polygenetic. Pebbles are mainly composed of sandstones and carbonate rocks and also large fragments of fossils with micrite envelope.

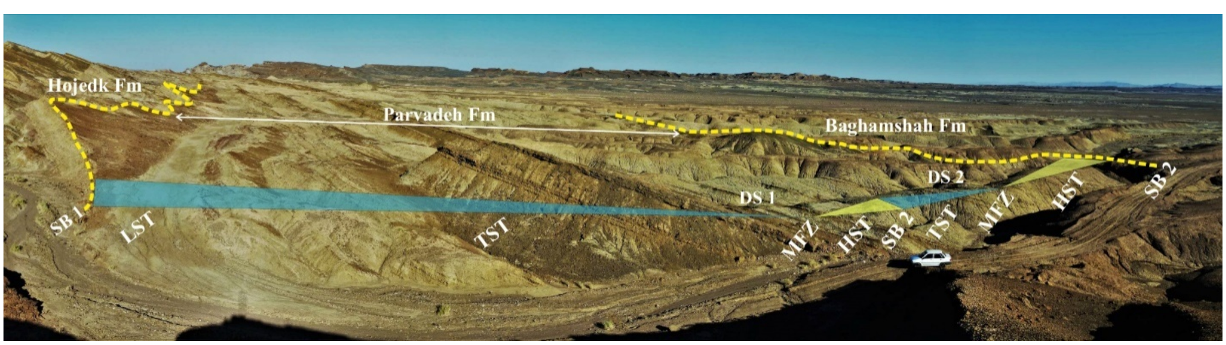

Figure 2. Characteristic outcrop of Middle Jurassic deposits of the Parvadeh Formation in the South of Parvadeh section that underlain Hojedk Formation and overlain by Baghamshah Formation.

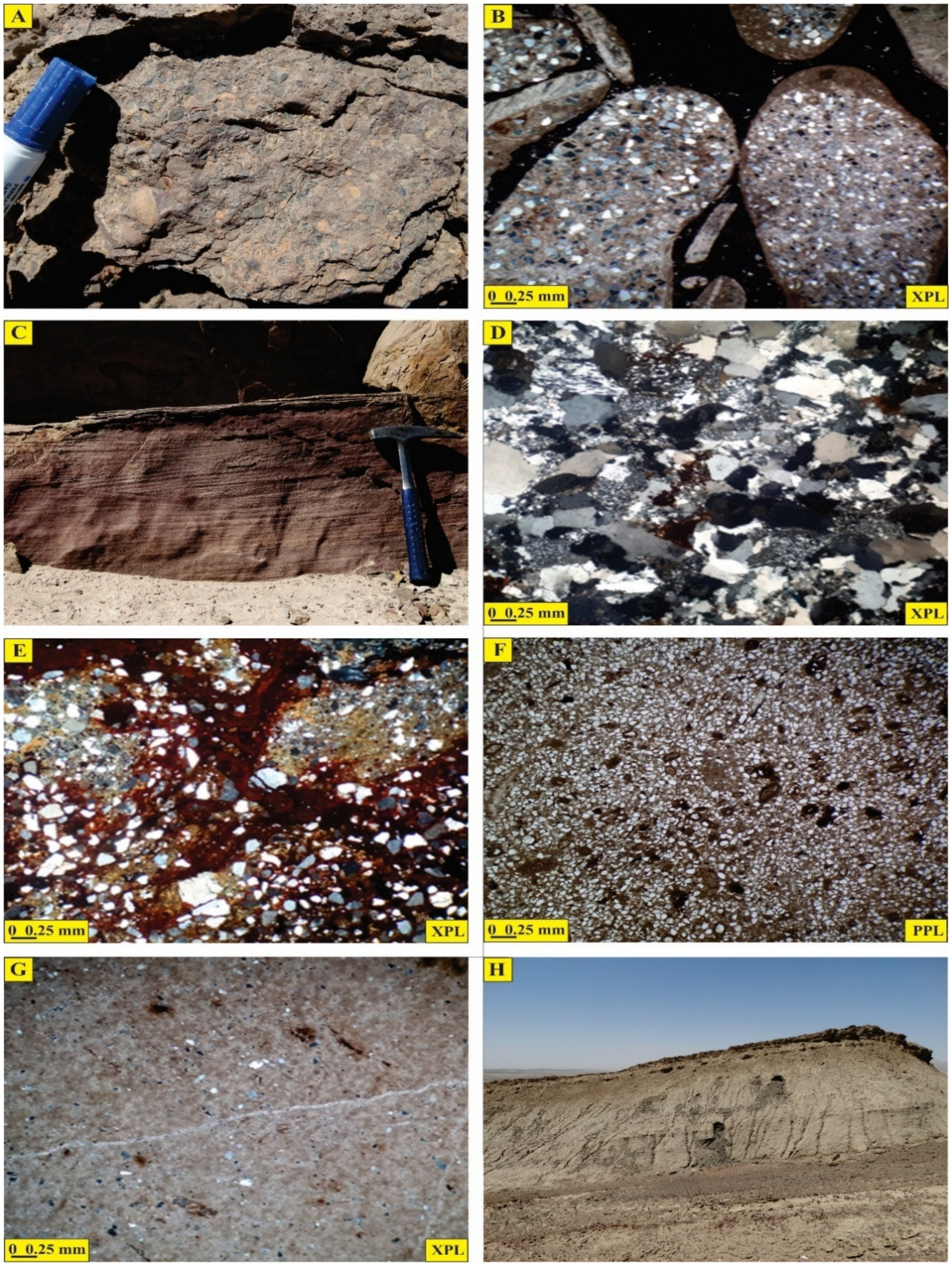

Figure 3. Tidal flat facies, A: Outcrop photograph of conglomerates in Parvadeh Formation (T1), B: Conglomerate having some sandstone and rounded bioclasts (T1), C: Outcrop photograph of sandstones showing planar and cross-bedding structures (T2), D: Sandstone with abundant chert fragments and moderate sorting (T2), E: Sandstone with abundant Fe oxide (T2), F: Sandstone with marine environment allochems (T2), G: Non fossiliferous mudrock with scattered quartz grains (T3), H: Outcrop photograph of grey to reddish shale and mud rocks (T3,T4).

The roundness of fragments in many parts represents the long transport distance and the effect of erosional factors on them. They are medium to thick-bedded red to brown color in the field. Pebbles are floated in a matrix of coarse sand with iron oxide and sometime carbonate cement (Fig. 3B). The size of conglomerate pebbles ranges between several millimeters to centimeters and shows the high energy of the environment and their probable formation in a channel high-energy environment which has been under the effect of the tidal currents.

Subfacies T2: Sandstone. Sandstones are the most frequent lithofacies in siliciclastic rocks of Parvadeh Formation that contain sedimentary structures such as ripple mark, planar and cross-bedding, relatively horizontal stratification and bioturbation (Fig. 3C). These sandstones have different grain sizes and forms which change between fine to coarse-grain, angular to subangular and sometimes rounded along the succession. These sandstones have relatively moderate sorting and roundness which are alternate with mud rocks lithofacies. Several types of sandstones including litharenite, sublitharenite, hybrid sandstone with fossils and marine allochems existed in the studied sections (Fig. 3D and F). Various grains, especially limestone fragments containing skeletal and non-skeletal allochems were observed in these sandstones which were cemented by calcite and Fe oxide and dolomite (Fig. 3E). Sedimentary structures such as lamination, cross-beds and ripples are present in this subfacies. These sandstones are grey to red in color in the outcrop.

Subfacies T3: Mudrock. This subfacies are often alternatively present with sandstone facies. Mud rocks in the studied sections are medium to thick bedded, mostly without fossil and sedimentary structure and sometimes with Fe-oxide contents (Fig. 3G and H). They sometimes display a distinct sub-millimeter-scale parallel lamination. They are thin to medium-bedded and grey to buff in color in the outcrop. Sand grains that are often quartz, can be sporadically observed in these mud rocks, in which their frequency reaches more than 10 percent. These mud rocks have been affected by several diagenetic processes, dissolution, neomorphism and compaction. Bioclast fragments are rarely sporadically observable in this facies. Calcite veins can be seen in some of the mud rocks which had been filled with the sparry calcite cement. This facies, which was deposited in the tidal area, especially the supratidal environment related to a carbonate ramp.

Subfacies T4: Shale. Shale beds are observed in the form of intercalates with sandstones and sometimes carbonated rocks and their thickness changes from a few centimeters to several meters (Fig. 3H). They have no fossil and are observed in red and grey color in the field. Their frequency is different in studied stratigraphic sections.

Interpretation (Siliciclastic Facies Association)

Considering the lack of fossils and their red color of shale and some sandstone and mud rock layers, they have been deposited in tidal flat and high-oxygen environment. Presence of sedimentary structures, such as cross-bedding, lens layers, flaser, trace fossils (Scolicia and Thalassinoides), planet fossils and presence of ripple marks confirm this interpretation (Fig. 4) (Adnan *et al.,* 2015; Patra & Singh, 2015; Sabbagh Bajestani *et al.,* 2017; Sim *et al.,* 2019). Also, the conglomerate with the intercalation of sandstones, which in many parts have a sedimentary structure such as cross and parallel stratification (Fig. 4) shows their formation in a channel and tide-dominated environments (Adnan *et al.,* 2015). Their limited extension and their lensed shape also confirm the channel conditions which eroded the lower part of these sediments due to the existence of currents at various times. Sublitharenite sandstones compared to quartz arenite, regarding the preservation of rock fragments, were formed in the environment with lower energy conditions and it can be argued that they have been less transported than quartz arenite (Tamura & Masuda, 2003). The presence of detrital sediments in different parts of the depositional environment at the time that there is potential for carbonate formation, indicates intense tectonic fluctuations in different parts of the environment (Miall, 2014). The conditions of sandstones formation are very different. In study sections, sandstones mostly belong to tidal environments due to lack of fossil, sedimentary structures and the presence of Fe-oxide (Hematite). Regarding the tectonic status of the area at the time of middle Jurassic (Wilmsen *et al.,* 2010), the components, sedimentary structures and low to moderate textural and compositional maturity of the studied sandstones, seem to be formed under the effect of river and sometimes marine currents. The sandstones can be deposited during the traction-suspension mechanisms (Khalifa & Catuneanu, 2008; Javidan *et al.,* 2015). Presence of Fe-oxide in the studied sandstones represents their deposition in the relatively shallow and oxygenated conditions.

Carbonate facies association

Lagoon facies (L1-L5)

Subfacies L1: Peloid wackestone/packstone.

Allochem in this subfacies includes mostly pellet and peloid, in which their frequency is about 30 to 60 percent. Fecal pellets are completely rounded and identifiable, but the peloids have various shapes and their origin can be mud rocks or other allochems crushing. In this subfacies, in addition to the peloids, there are skeletal grains such as bivalve, gastropod, foraminifera and algae. Also, sand grains, which are mostly quartz, have sometimes a considerable frequency and show the coastal currents carrying the sand grains to the environment (Fig. 5A).

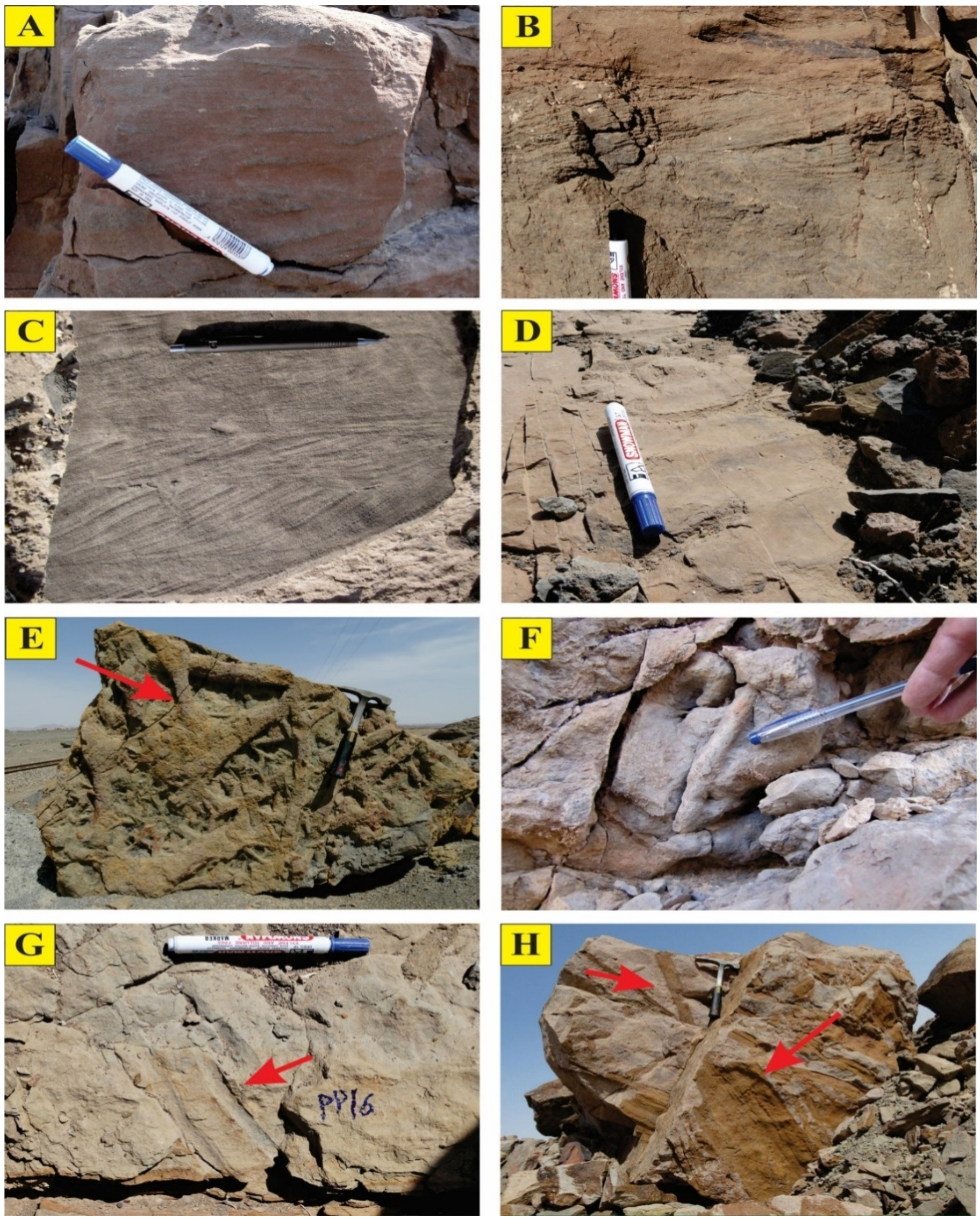

Figure 4. Field photo of sedimentary structures and trace fossils of Parvadeh Formation deposits in the studied sections, A: Flaser bedding in Mazino section, B: Planar cross-bedding in sandy limestone on Kalshaneh section, C: Planar and trough cross-bedding in the sandstones of Mazino section, D: Ripple marks in Mazino section, E: Thalassinoides trace fossil in Chah-e-Kamardoshakh section, F: Thalassinoides trace fossil in Kalshaneh section, G: Scolicia trace fossil in tidal flat facies of Parvadeh Formation in south of Parvadeh section, H: Planet fossils in Chah-e-Kamardoshakh section.

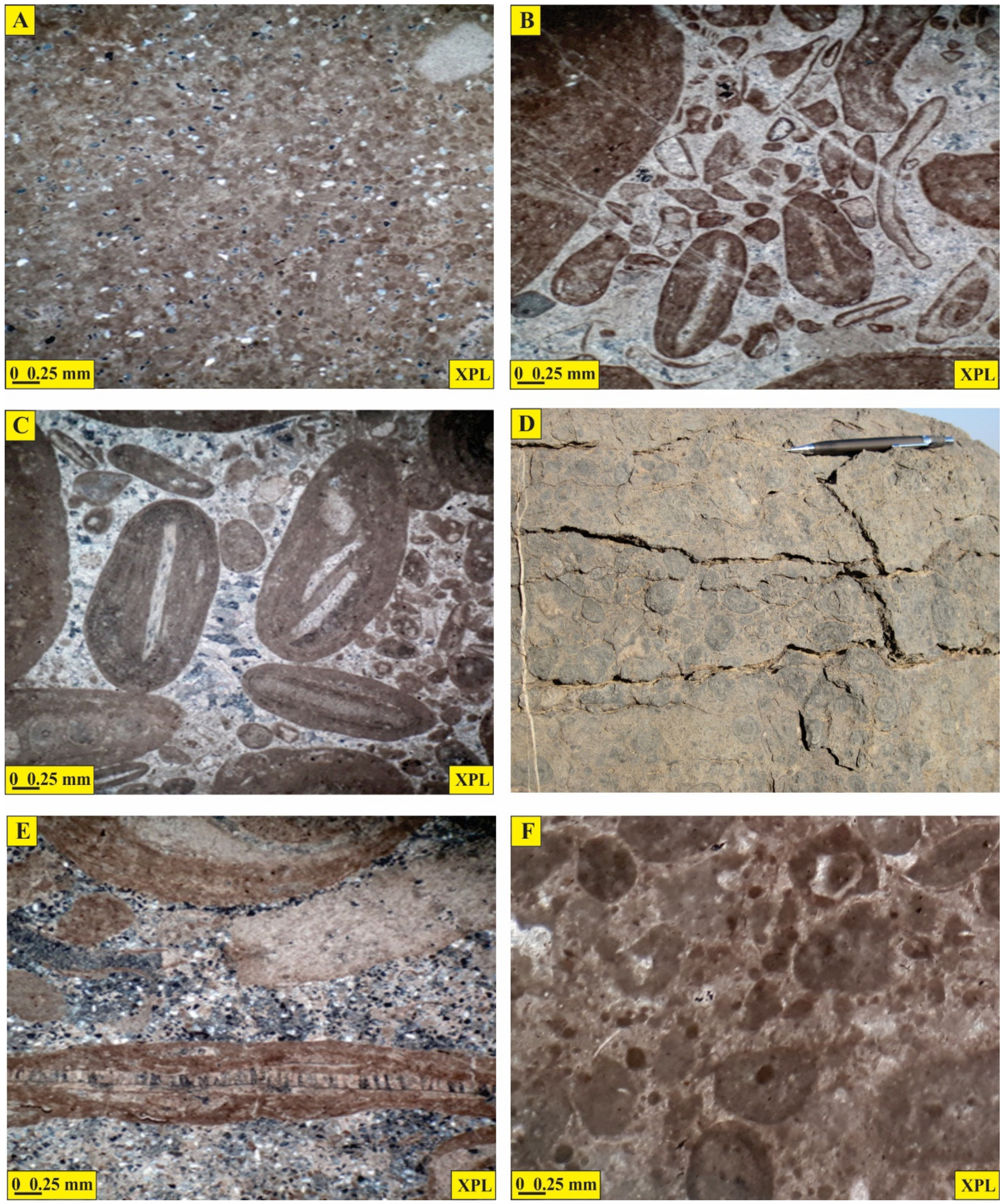

Figure 5. Lagoon facies, A: Peloid wackestone/packstone subfacies and sand particles are mostly formed of quartz (L1), B: Bioclast intraclast oncoid grainstone subfacies (L2), C: Oncoid packstone/grainstone subfacies (L3), D: Field photo of oncoid packstone/grainstone subfacies (L3), E: Bioclast oncoid grainstone/packstone subfacies (L4), F: Intraclast packstone subfacies with various size of intraclasts (L5).

Compaction in some parts causes a change in the shape and orientation of pellets. This subfacies is light grey to grey in color with lamination in the outcrop.

Subfacies L2: Bioclast intraclast oncoid grainstone. Allochems existing in this subfacies consist of oncoid, intraclast and bioclast. Size of oncoid varies and ranges from 0.2 millimeter to several centimeters. Oncoids of this subfacies are more abundant than other allochems and their size is larger than other allochems like bioclast, intraclast. Bioclasts are normally bivalve particles and sometimes gastropod and foraminifera fragments (Fig. 5B). They are medium to thick bedded, grey in color and sometimes with lamination in the field.

Subfacies L3: Oncoid packstone/grainstone. There are oncoids with various forms and sizes in this subfacies. The form of oncoids is mostly influenced by the type of core and oncoids with bioclast core can be seen in elongated form. Other skeletal and non-skeletal allochems including ooid, intraclast, milliolid and bivalve are observed in this subfacies. In this subfacies, the space between allochems is filled with micrite and in place with sparry calcite cements. Oncoids in some layers have very large sizes and are clearly observed in the outcrop (Fig. 5C and D).

Subfacies L4: Bioclast oncoid grainstone/ packstone. In this subfacies, oncoid is more abundant than other allochems and interparticle space is filled with sparry calcite cement, especially blocky and drusy calcite. Other allochems, such as peloid and low amounts of intraclast and sometimes ooid are observable with oncoids (Fig. 5E). The edges of many intraclasts are rounded which suggest their transport by currents to this place. Low amount of skeletal debris consisting of bivalve and foraminifera are present in this subfacies, which are affected by micritization in some parts. These limestones are medium-grained, grey colored, medium- to thick-bedded but in places laminated.

Subfacies L5: Intraclast packstone. The main allochem of this subfacies is intraclast (about 45-50%) with different size and forms which are sometimes well-rounded but poorly sorted mud fragments (Fig. 5F). Other non-skeletal allochems such as oncoid and peloid are observed in this subfacies. Oncoids size varies from 1 to >2 mm with nuclei of other allochems such as bioclast and intraclast. Bioclasts in this subfacies mostly consist of gastropod, foraminifera and bivalve fragments with different frequencies. In the field, this rock type appears fine- to medium-grained, grey-colored and medium to thick-bedded (1–3 m). The spaces between allochems are filled with lime mud affected by diagenesis process (neomorphism, compaction and dissolution).

Interpretation (Lagoon Facies)

These facies are often composed of skeletal and non-skeletal allochems (gastropod, framinifera, pellet, peloid and oncoid) that belong to low energy and restricted environments. But some of allochems belong to other environments that probably have been carried by currents. Regarding the fact that pellets are formed in warm and supersaturating water of calcium carbonate (Bjørlykke, 2010), they indicate deposition in the back shoal low-energy lagoon environment with no effects of sea waves (Burchette & Wright, 1992; Adachi *et al.,* 2004; Sabbagh Bajestani *et al.,* 2017). Large amounts of peloid with lime mud in many facies represent their sedimentation in low-energy lagoon environment (Adachi *et al.,* 2004). Also presence of micrite between allochems shows the formation of these facies in a shallow and low-energy lagoon environment (Cadjenovic *et al.,* 2008). Texture with weak sorting and allochems micritization and presence of lagoon bioclasts with normal marine bioclasts show their formation in a semi-limited lagoon environment (Hallock & Glenn, 1986). Also, presence of abundant oncoids in many of these facies proves their formation in a low-energy and lagoon environment. In general, on the basis of the existence of lagoonal bioclasts such as milliolid and their accompaniment with tidal flat facies, the presence of micrite between particles, development of micritization process and bioturbation, these facies belong to lagoon environment (Geel, 2000; Alsharhan, 2006; Maurer *et al.,* 2009; Badenas & Aurell, 2010; Flügel, 2010; Adabi *et al.,* 2010; Berra *et al.,* 2019). Oncoidal facies are also sometimes attributed to tidal channel deposits adjacent to the ooid shoals (Adams & Diamond, 2019).

Shoal facies (S1-S6)

Subfacies S1: Ooid grainstone. The main allochem in this subfacies is ooid which can be seen in various forms and sizes. The forms of ooids are radial, superficial, extended and compound and their clasticity index ranges from 0.5 to 1.5 Pore and interparticle spaces were filled with different types of sparry calcite cements including equant, drusy, isopachous and sometimes poikilotopic cement. Bivalve, brachiopoda, coral and echinoderm fragments and also non-skeletal components, including intraclast, oncoid and peloid with a lower frequency, can be observed in this facies (Fig. 6A). This subfacies had relatively good textural maturity, roundness and well sorting. They are dark grey to grey in color and medium to thick-bedded sometime with cross-bedding.

Subfacies S2: Intraclast ooid grainstone. Ooid and intraclast are the most abundant allochems in this subfacies and between allochems has been filled with sparry calcite cement and in some parts with a lower amount of micrite. Sand grains, which are mostly quartz, are scattered in this subfacies and sometimes form the core of ooids. Intraclast is almost abundant and their clasticity indices are higher than ooids and also have moderate sorting and roundness. Many of ooids are under the effect of micritization process and usually their internal structure has been destroyed (Fig. 6B). This subfacies is buff to grey in color and relatively thick-bedded with planar cross-bedding.

Subfacies S3: Sandy bioclast ooid grainstone. Ooids and bioclast form the main allochems of this subfacies. The frequency of ooid is more than bioclasts and different types of ooid exist in this subfacies which are often affected by micritization.

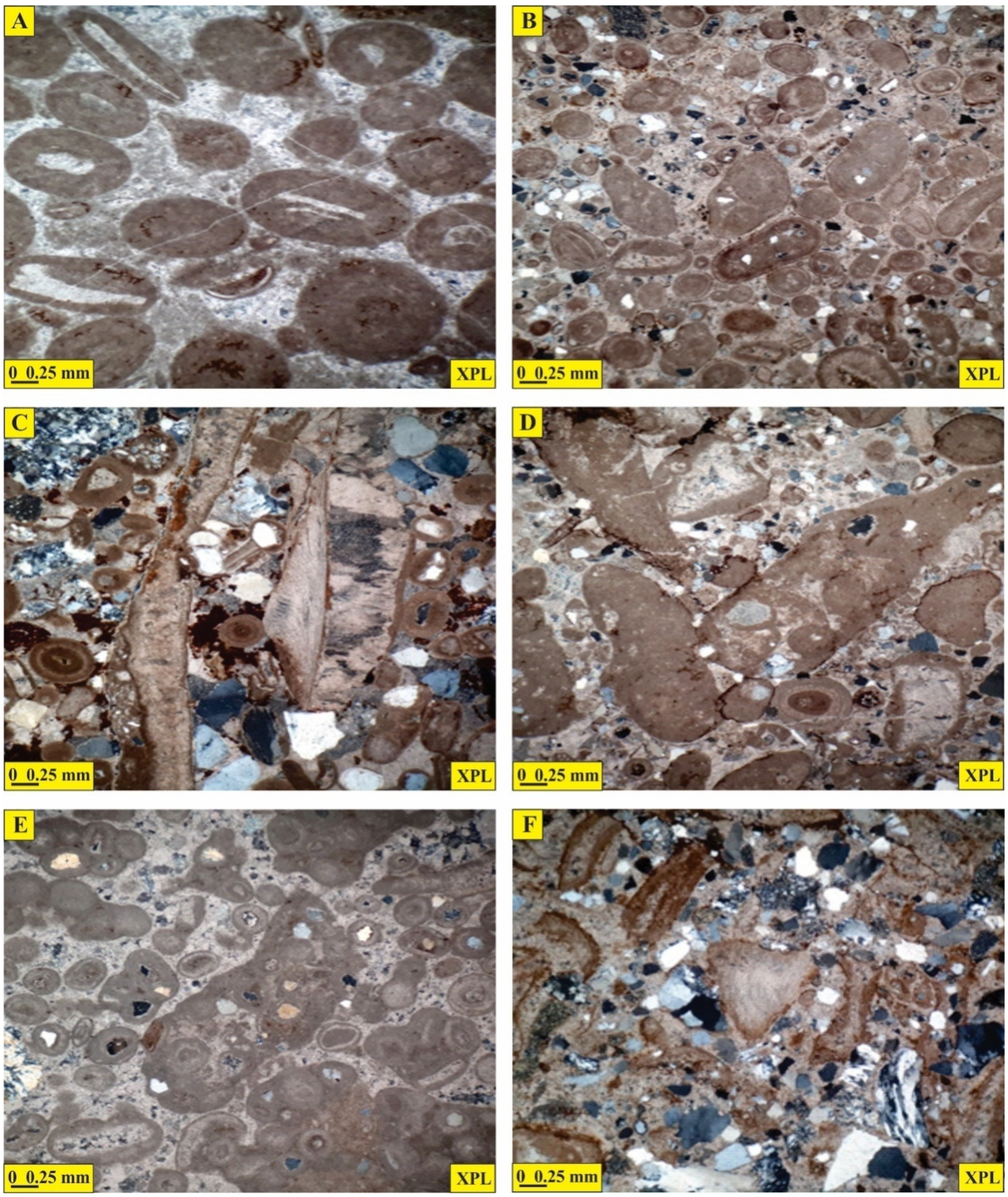

Figure 6. Shoal facies, A: Ooid grainstone subfacies (S1), B: Intraclast ooid grainstone subfacies (S2), C: Sandy bioclast ooid grainstone subfacies (S3), D: Intraclast grainstone subfacies (S4), E: Ooid intraclast grainstone subfacies (S5), F: Sandy bioclast grainstone subfacies (S6).

Bioclasts are mostly consisting of bivalves and brachiopoda. In some parts, diagenetic processes such as dissolution and silicification influenced some allochems. Quartz grains are sporadically observable between allochems and between them had been filled mainly with sparry cement and lower amount of micrite and Fe oxide (Fig. 6C). In the field, this subfacies is medium to thick-bedded with cross-bedding and sometime bioclasts that observed in the surface of layers.

Subfacies S4: Intraclast grainstone. This subfacies is abundant in the studied sections and contains intraclasts with various dimensions and sizes. Size of intraclasts is more than two millimeters in some of the studied samples and had been formed with the crushing of previous rocks. In this subfacies, in addition to intraclasts, skeletal components including bivalve, coral, gastropod, echinoderm, brachiopod and non-skeletal components such as ooid and peloid are observable. The clasticity index of intraclasts would reach up to 2 millimeters in this subfacies (Fig. 6D). Some of the intraclasts are more angular and some have rounded edges. In the field, the beds appear as dark grey, medium to thick-bedded, cross-bedded and laminated calcarenites.

Subfacies S5: Ooid intraclast grainstone. This subfacies is found in many of the studied sections and there are intraclasts with different sizes and relatively low sorting. There are ooids with a high frequency inside most of the intraclasts. Between allochems is filled with various types of sparry cements such as blocky, drusy, granular and sometimes poikilotopic. Size of intraclasts ranges from less than 0.5 mm to more than 2 mm in which, size and type varies in different sections (Fig. 6E). This subfacies appears as medium-grained, grey, thick-bedded (about 2–3 m) cross-bedded calcarenites.

Subfacies S6: Sandy bioclast grainstone. Bioclast grainstone subfacies are one of the most abundant available subfacies in the studied sections. Small to large-size skeletal components consist of coral, bivalve, echinoderm, brachiopod, gastropod with a lower amount of bryozoans are exist in this subfacies (Fig. 6F). Coral fragments, bivalve, brachiopod are larger than the other components and this fossil can be separately seen in the outcrop. The non-skeletal components such as intraclast, ooid and peloid can be seen between the skeletal components with a different frequency. The beds are grey, medium to thick-bedded with fossil fragments.

The space between allochems has been filled by different types of sparry cement. Some of the allochems such as ooids and skeletal grains had been affected by micritization and their primary structure has been destroyed. Some diagenetic processes like dissolution and replacement can also be seen in some parts.

Interpretation (Shoal Facies)

Well-washed grain-supported grainstones with sparry calcite cement show shallow marine high energy conditions. Absence or low amount of micrite between allochems shows the continuous flow of water and consequently washed-up micrite (Flügel, 2010; Koehrer *et al.,* 2010; Bover-Arnal *et al.,* 2009; Bayet-Goll *et al.,* 2018). The roundness of the main components and their moderate to good sorting could reflect shallow-water high-energy bioclastic shoals environment (Pleş *et al.,* 2019).

Availability of open marine skeletal allochems such as echinoderm, coral and brachiopod in the ooid and intraclast grainstone facies shows the deposition of these subfacies in shoal areas towards the open marine (Flügel, 2010). Peloid is also one of the other important components of these facies. The existence of peloid with granular sparry calcite and drusy cement represent their movement from the low-energy to high-energy environment and then deposition in high-energy shoal environments (Carozzi, 1989; Sinclair *et al.,* 1998). Bryozoan fragments also exist in some of the subfacies. Regarding that Bryozoan can usually live and grow in low light conditions, in addition to the existence of micrite between grains and lack of red algae, it can be concluded that this facies was formed in a low energy oligophotic and mesophotic environment (Pomar, 2001). The frequency of echinoid in many subfacies shows their formations in open marine environments (Flügel, 2010). However, in some of the subfacies, there are some lagoonal bioclasts which have probably been carried to this environment by currents. The dominance of moderate to high abrasion and fragmentation of macrofossil shells, their horizontal concave-down arrangement and coarse size of the bioclasts indicate high-energy selective transport (Armenteros *et al.,* 2019). Biclaste ooid grainstone subfacies represent shoal and shoal to lagoon environment with high energy conditions (Flügel, 2010; Koehrer *et al.,* 2010; Pleş *et al.,* 2019). Ooid grainstone is related to shoal environment and indicates sedimentation in FWWB (Alsharhan, 2006; Maurer *et al.,* 2009; Koehrer *et al.,* 2010; Bai *et al.,* 2017).

Open marine facies (O1-O3)

Subfacies O1: Bioclast wackestone/packstone. Bioclast components in this subfacies consist of brachiopod, bivalve, echinoderm, coral and sometimes lower amount of gastropod and foraminifera. Micrite filled the space between grains and sometimes compaction caused the compression of allochems and created suture contact. Bioturbation could be sporadically observed in this subfacies which was filled by micrite. The rocks are medium to thick-bedded, light grey to grey-colored and sometimes bioclast are observed in the hand sample. Micritization affected some of the bioclasts, especially echinoderm fragments (Fig. 7A and B).

Dissolution of the bioclasts in some parts shows the aragonite and calcite with high magnesium composition of them which have high solubility (Farry & Van Hassel, 2007). This process can be seen in bivalve and gastropod fragments.

Subfacies O2: Peloid wackestone. Peloid and bioclast are the main allochem in this subfacies and the space between them is filled with micrite. Sporadic bioclasts in this facies consist of echinoderm, brachiopod and bivalve. Bioclasts in this facies consist of open marine fauna such as echinoderm, brachiopod and bivalve. Bioturbation can be seen in this subfacies and sometimes the clastic grains which are mostly quartz are observable (Fig. 7C). They are gray to buff in color, medium- to thick-bedded, mostly non laminated and homogeneous.

Subfacies O3: Mudstone. This subfacies has a low amount of bioclast (about 2 to 6 percent), consisting of small fragments of brachiopod, bivalve and sponge needle and sometimes echinoderm, belemnite and ammonite (Fig. 7D).

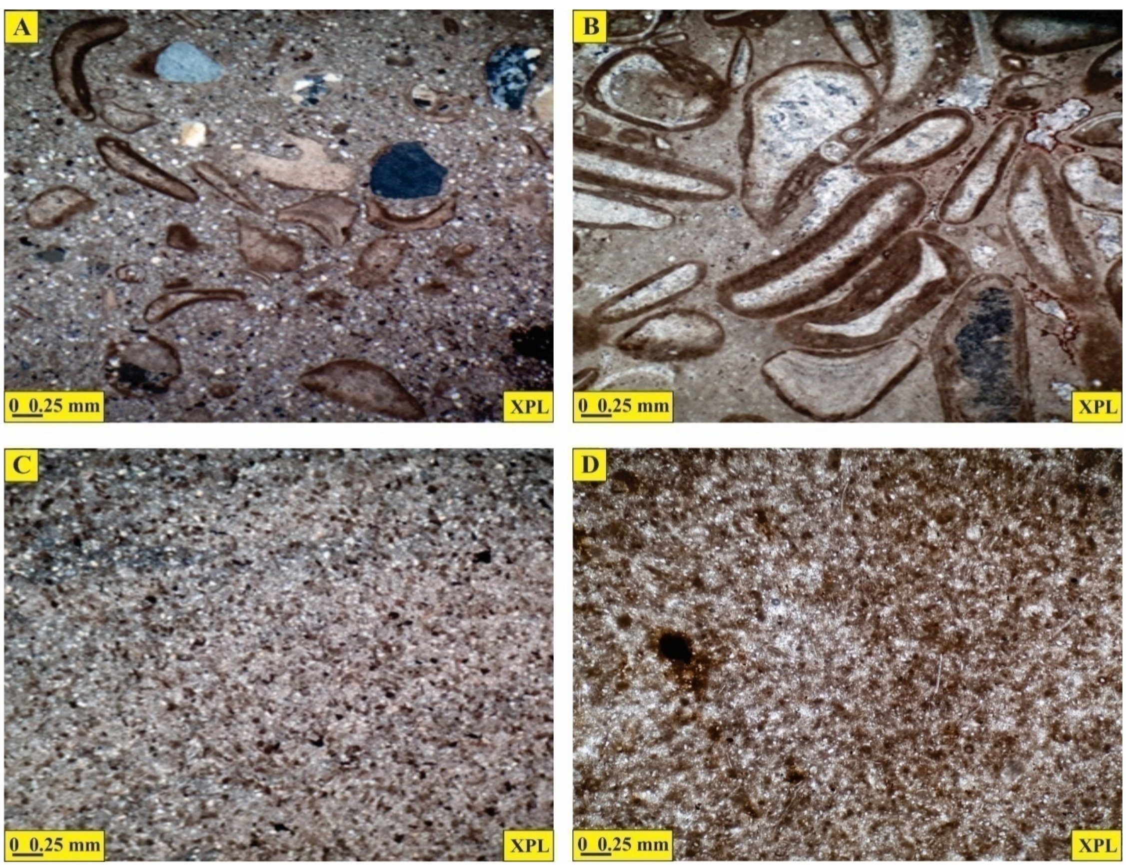

Figure 7. Open marine facies, A: Bioclast wackestone subfacies with brachiopoda, echinoderm and bivalve fragments (O1), B: Bioclast packstone subfacies (O1), C: Peloid wackestone subfacies (O2), D: Mudstone subfacies (O3).

Lamination and low amount of bioturbation can be observed in this subfacies. Mudstones are light grey to grey, thin-bedded, laminated and with low fossils in the field.

Interpretation (Open marine Facies)

These subfacies mostly contain open marine skeletal allochems and fossils such as echinoderm, brachiopod, coral and low amount of bryozoan, belemnite, ammonite and sponge needles. Considering the low energy in this environment, the space between allochems is mostly filled with micrite. Presence of lamination in the rocks of this facies assemblage shows slow energy conditions at the time of deposition. Based on the abundance of Stenohaline fauna, including bryozoa and echinoderms and abundant mud, this facies was possibly deposited in a low energy environment below the fair weather wave base (Bachmann, & Hirsch, 2006; Flügel, 2010). Many of the ramp facies that deposited in the photic zone typically consist of crinoid, brachiopod, bryozoan, and bivalve (Burchette *et al.,* 1990; Bai *et al.,* 2017).

Wackestone facies, with sponge needle are one of the many facies which have sedimented in a quiet marine environment. Also the presence of high amount of micrite shows a quiet and low-energy environment. Depositional environment of mudstone subfacies, considering its properties is outer ramp (Wilson, 1975; Cluff, 1984; Adachi *et al.,* 2004; Bover-Arnal *et al.,* 2009; Berbier *et al.,* 2012). In the deep marine environment due to the low energy conditions and low rate of sedimentation, there are just fine-grained sediments with transferred allochems and clastic-bioclasts which are related to the shallow marine environment. In addition, some sediment is transferred to the environment by the wind (Haq, 1991; Hueneke & Mulder, 2011).

Depositional Model

According to the performed investigations, the identified facies have deposited in tidal flats, lagoon, shoal and open marine environments. These facies have gradually transformed to each other in many parts and no abrupt change is observed. Some of the quick shifts can be due to the erosional factors which occurred by the currents. On the basis of the absence of frame-building creatures such as coral, presence of abundant amounts of ooid grainstones, gradual change in facies and their no-sudden change, a carbonate ramp model is proposed for the study deposits (Burchette & Wright, 1992; Elgadi & Brookfield, 1999; Brachert *et al.,* 2001; Pomar, 2001; Aurell *et al.,* 2003; Corda & Brandano, 2003; Bai *et al.,* 2017). In the studied facies, there are some corals which belong to patch reef and are formed in the ramp environment (Ehrenberg *et al*., 2002; Alsharhan, 2006) (Fig. 8).

Sequence stratigraphy

Sequence stratigraphy includes identification and correlation of changes in depositional trend of the rock successions (Embry, 2002). Identification and analysis of depositional sequences and sea level changes were done according to Van Wagoner *et al.,* (1988, 1990) and Catuneanu *et al.,* (2009, 2011, 2013) and were accurately performed in all sections. Factors such as performance between the amount of sediment supply, basin floor physiography and relative changes of sea level, controlled and affected sediments deposition and their temporal as well as spatial expansion. Relative changes in sea level are controlled by both of eustatic fluctuations and subsidence or uplift of basin floor (Ketzer, 2002). Various factors such as lithology, sedimentary structures and textures, microfacies and lateral changes in microfacies can help to identify depositional sequences (Catuneanu *et al.,* 2009, 2011, 2013; Yilmaz & Altiner, 2007). In this study, two third-order depositional sequences and sea water level fluctuation were identified by detail facies studies and compilation of field and microscopic evidence. These two sequences were precisely investigated in studied sections and are discussed as follow.

Depositional Sequence 1 (DS1)

In Kal-e-Shur section, the lower boundary of this sequence with the Hojedk Formation is erosional (SB1) and the sandstones of Parvadeh Formation are located on the shale and sandstones of Hojedk. These sandstones are mostly litharenite and sublitharenite and after them, sandy bioclast ooid grainstone of shoal environment are deposited due to the sea level transgression. After that during sea water transgression, open marine bioclast ooid packstone facies has been deposited and formed maximum flooding zone (MFZ). Then sea water regression has occurred and highstand system tract (HST) deposited. The thickness of the first sequence in Kal-e-Shur section is about 33 meters. The boundary of this sequence with the DS2 is due to the presence of erosional evidences of the sequence boundary type 1 (SB1) (Fig. 9 and 10). In Mazino section, the first sequence boundary with Hojedk Formation is erosional type and the red conglomerates of lowstand system tract (LST), are located on Hojedk Formation deposits. After that, the sea water transgressed and sand intraclast bioclast grainstone facies, ooid grainstone and bioclast ooid intraclast grainstone of transgressive system tracts (TST) were deposited. Maximum flooding zone is formed by deposition of in traclast bioclast packstone facies and then highstand system tact deposits HST, including shoal facies was formed. The thickness of this sequence is almost 40 meters and the upper boundary of this sequence with the second sequence DS2 is SB2 type (Fig. 11). In the Chah-e-Kamardoshakh section (Abbas Abad), DS1 is located on the Hojedk Formation deposits with erosional boundary (SB1). This sequence begins with sandstone facies, belonging to tidal flats and continued with a slow transgressive and formation of TST deposits.

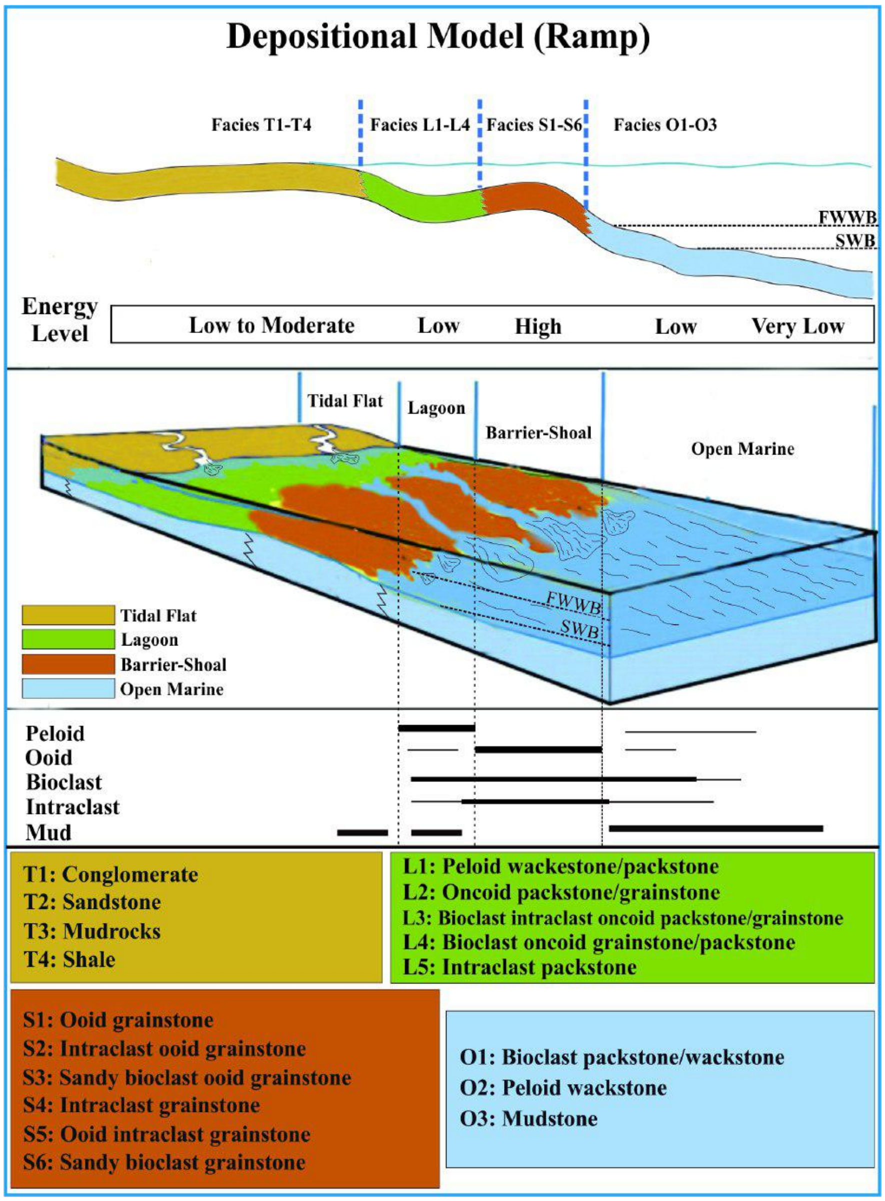

Figure 8. Ramp model of Parvadeh Formation deposits. Based on facies and their lateral and vertical changes, a ramp model is proposed for the Parvadeh Formation. These facies was formed in tidal flat to open marine environment.

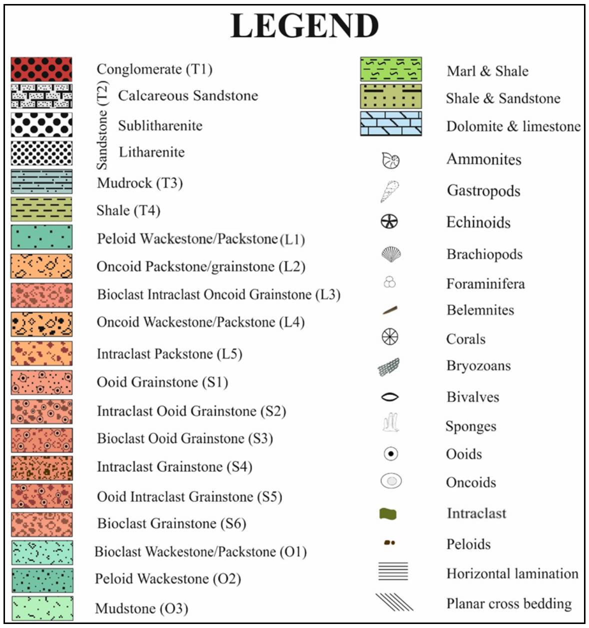

Figure 9. Signs used for skeletal and non-skeletal allochems, facies, sedimentary structures in sequence stratigraphy column, Figures 10 to 15.

Maximum flooding zone was formed by deposition of bioclast and intraclast ooid grainstone subfacies belonging to shoal environment on the tidal and lagoon facies. Then, sea level has been relatively stable and the lagoonal facies of HST has been deposited. These facies mainly consist of biolclast packstone containing pellet and intraclast and sandy bioclast oncoid wackestone/packstone. The thickness of this sequence is about 17 meters (Fig. 12). In the south of Parvadeh section with 80 meter thickness, two third-order depositional sequences were identified considering the facies changes and sea level fluctuations. Sequence one (DS1), with a 38-meter thickness, is formed of LST, TST, and HST. The lower boundary of the sequence is erosional type (SB1), which includes conglomerate in its base and is erosionally located on the Hojedk Formation facies. LST is mainly formed of conglomerate and sandstone and shales related to tidal flat in the base of sequence, showing the sea level fall in the upper boundary of Hojedk Formation and after that, sea level beginning to transgressive. After deposition of these facies, sea level transgression started and carbonated facies of lagoon and shoal environments, including wackestone, packstone and bioclast, intraclast and ooid grainstones with low amounts of oncoid, deposited on the mainly clastic facies of tidal flats. Maximum flooding surface mainly includes grainstone subfacies, related to the shoal environment, after which the sea has fewer fluctuations and HST is formed with deposition of shoal and lagoon facies. The boundary of this sequence with the second sequence (DS2) due to the absence of erosional evidence is considered as sequence boundary type 2 (SB2) (Fig. 13). In the Sikhuri section, the first sequence (DS1) is located with an erosional boundary and angular unconformity on the limestones and dolomites of Jamal Formation. This sequence begins with high energy and shoal facies consisting of intraclast ooid grainstone, calcareous sandstones, bioclast ooid grainstone and after the marine transgression, shoal and open marine facies, such as sandy ooid bioclast grainstone/packstone and intraclast ooid packstone/grainstone of TST have deposited. Maximum flooding surface in this sequence includes open marine facies (ooid bioclast grainstone/packstone). After the transgression, HST has deposited with formation of the shoal and channel facies, showing the gradual regression of sea level and based on channel facies formation, the boundary of this sequence with the second depositional sequence (DS2) is erosional (SB2) (Fig. 14). The lower boundary of this sequence with Hojedk Formation in Kalshaneh section is erosional type SB1 and the red conglomerates in its base make LST facies. After this system tract facies, tidal flat sandstones and mudstones, and in the following shoal intraclast ooid grainstone facies were deposited and formed TST. Maximum flooding zone (MFZ) was formed by deposition of open marine bioclast wackestones containing bioclasts and then, with deposition of shoal and tidal flat deposits, highstand system tract (HST) was formed. The thickness of this sequence is about 22 meters and its boundary with the upper sequence is of non-erosional type (SB2) (Fig. 15).

Depositional Sequence 2 (DS2)

Second sequence in Kal-e-Shur section begins with deposition of tidal flat sandstones and continues by transgression of the sea level and deposition of the lagoon and shoal facies (TST). Maximum flooding zone in this sequence is formed by shoal intraclast bioclast grainstone subfacies. HST in this sequence is mostly formed of lagoonal facies which its upper boundary with shale and marl facies of Baghamshah Formation is SB2. (Fig. 10). In Mazino section, this sequence is mostly consisting of lagoonal oncoid/peloid wackestone/packstone subfacies and shows low sea level fluctuations, gradual transgression and formation of TST facies. Maximum flooding zone (MFZ) in this sequence consists of shoal intraclast grainstone/packstone subfacies. Highstand system tracts (HST) in this sequence, mostly consists of lagoon facies located below Baghamshah Formation with a type 2 sequence boundary (SB2) (Fig. 11). In Chah-e-Kamardoshakh (Abas Abad), this sequence is situated on the sequence one with a non-erosional boundary SB2.

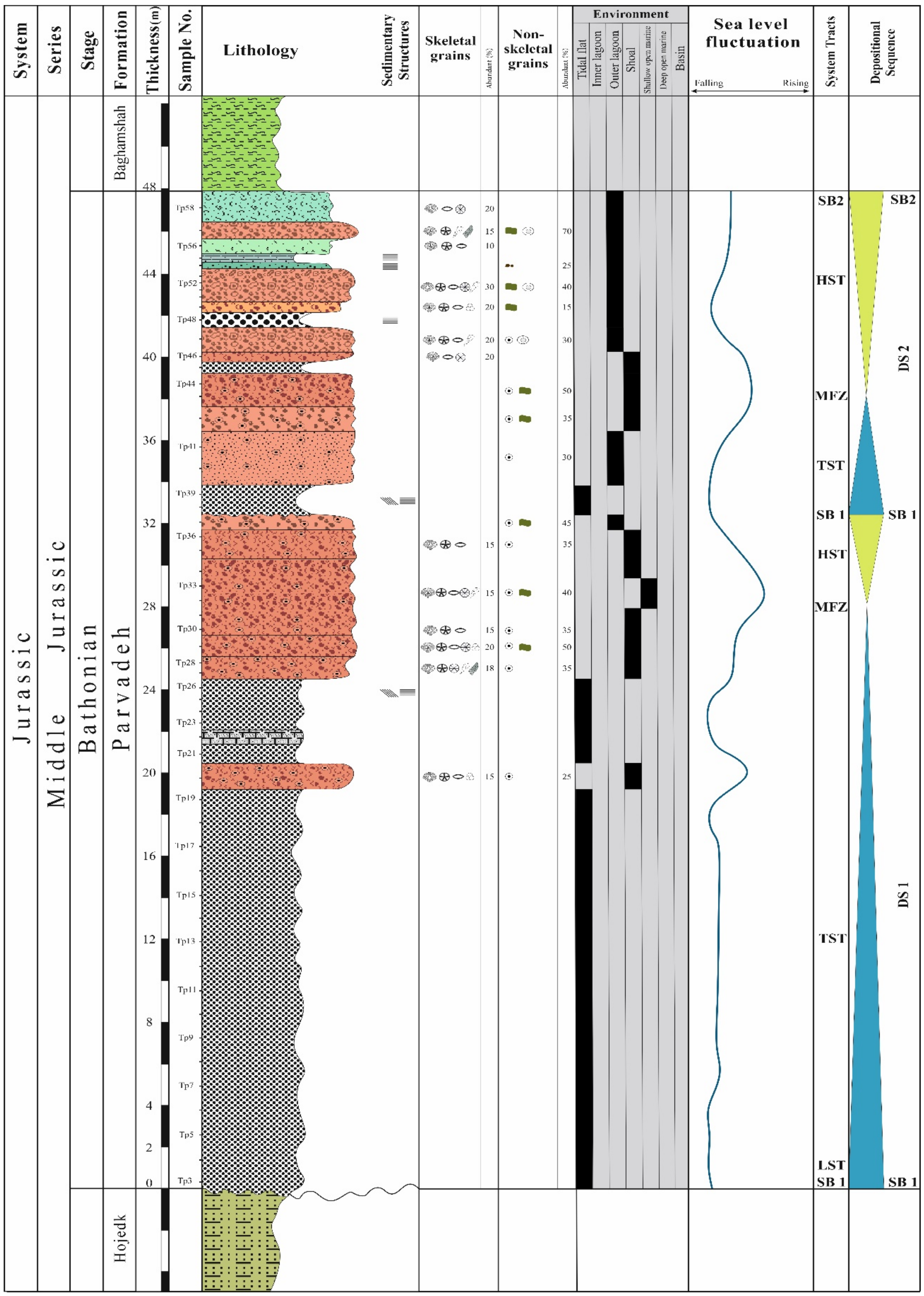

Figure 10. Sequence stratigraphy of Parvadeh Formation in Kal-e-Shur section.

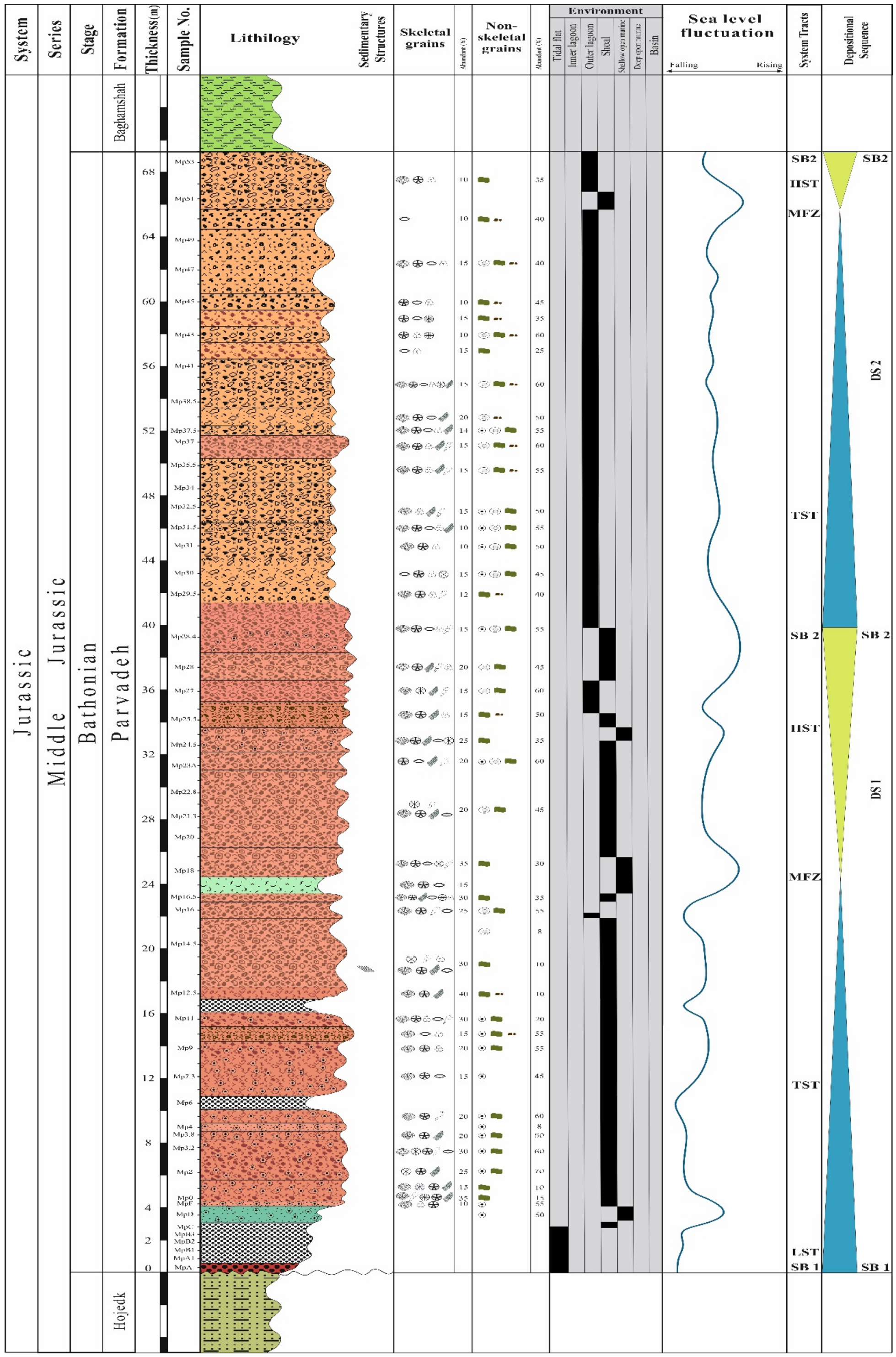

Figure 11. Sequence stratigraphy of Parvadeh Formation in Mazino section.

In the following, the lagoonal facies including bioclast intraclast packstone with low amounts of oncoid, oncoid intraclast packstone, pellet intraclast packstone with oncoid, are deposited and during transgressive of sea level, shoal facies, including intraclast grainstone/packstone with bioclast are deposited and form maximum flooding zone (MFZ). Finally, the sea started to regress and the lagoon facies of HST were deposited. This sequence gradually with non-erosional boundary located below the shale and marl deposits of Baghamshah Formation. The thickness of this sequence is 36 meters (Fig. 12). In South of Parvadeh section, sequence two (DS2), with 42-meter thickness, is deposited on the sequence one (DS1) with non-erosional boundary.

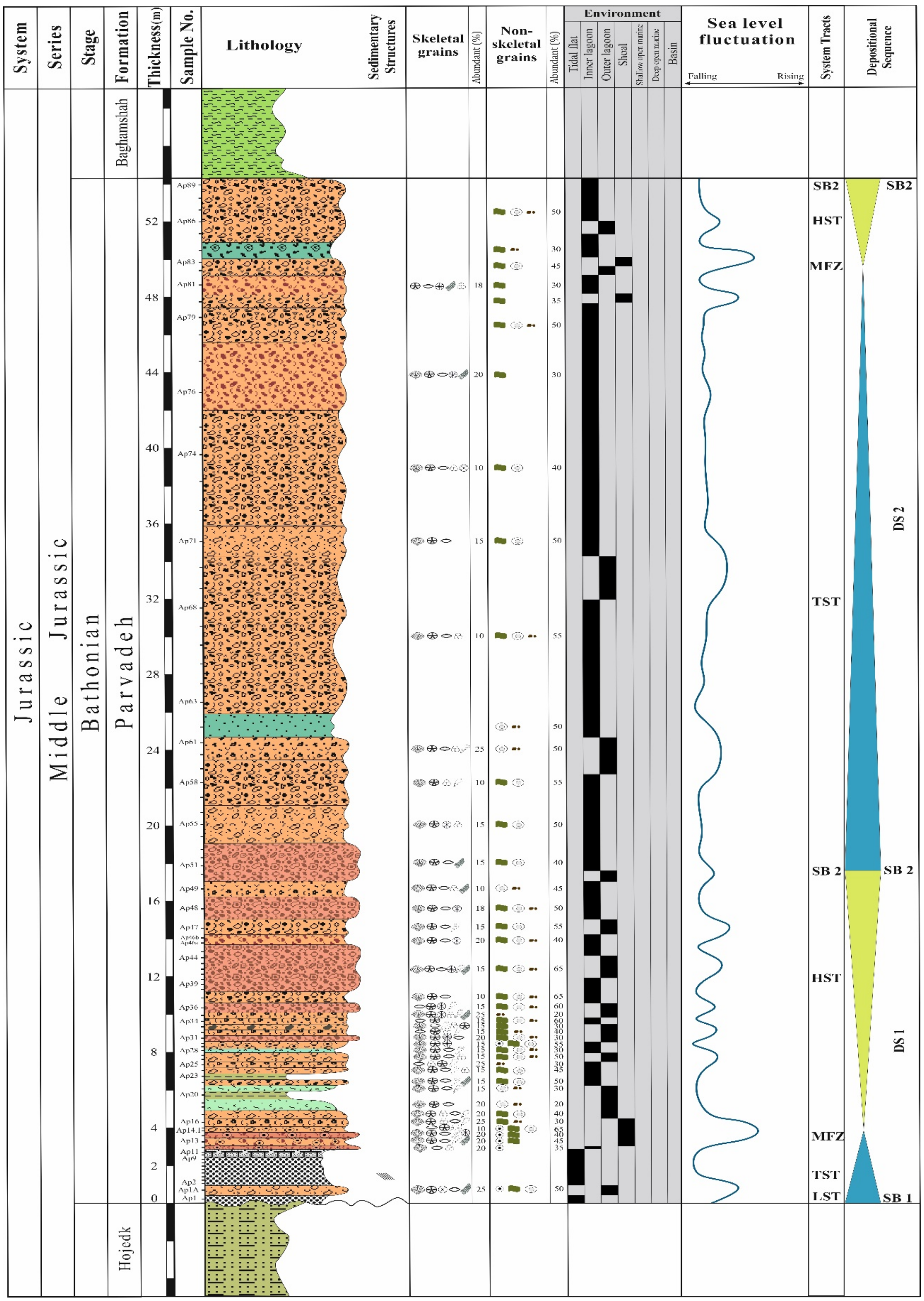

Figure 12. Sequence stratigraphy of Parvadeh Formation in Chah-e-Kamardoshakh (Abbas Abad).

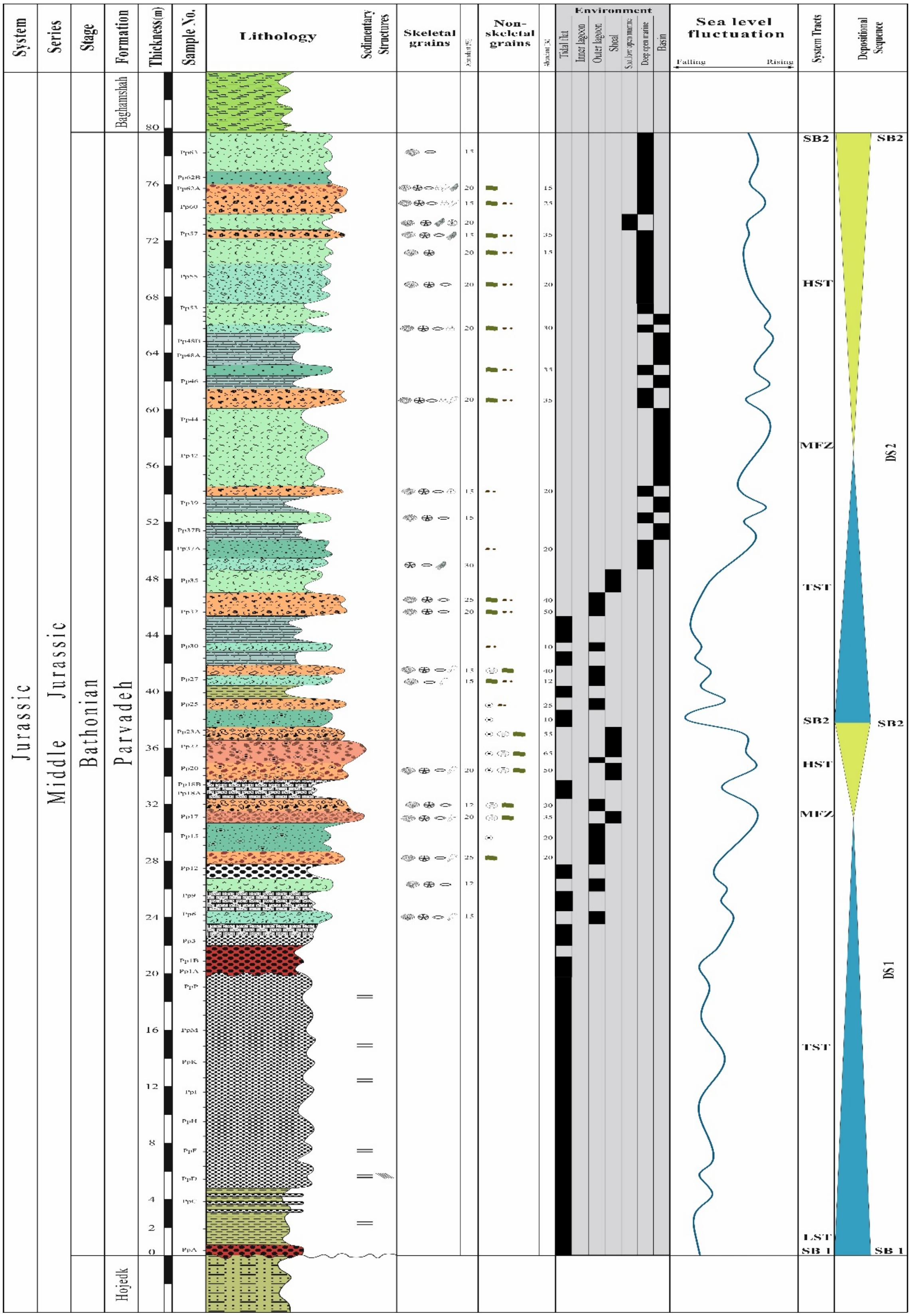

Figure 13. Sequence stratigraphy of Parvadeh Formation in south of Parvadeh section.

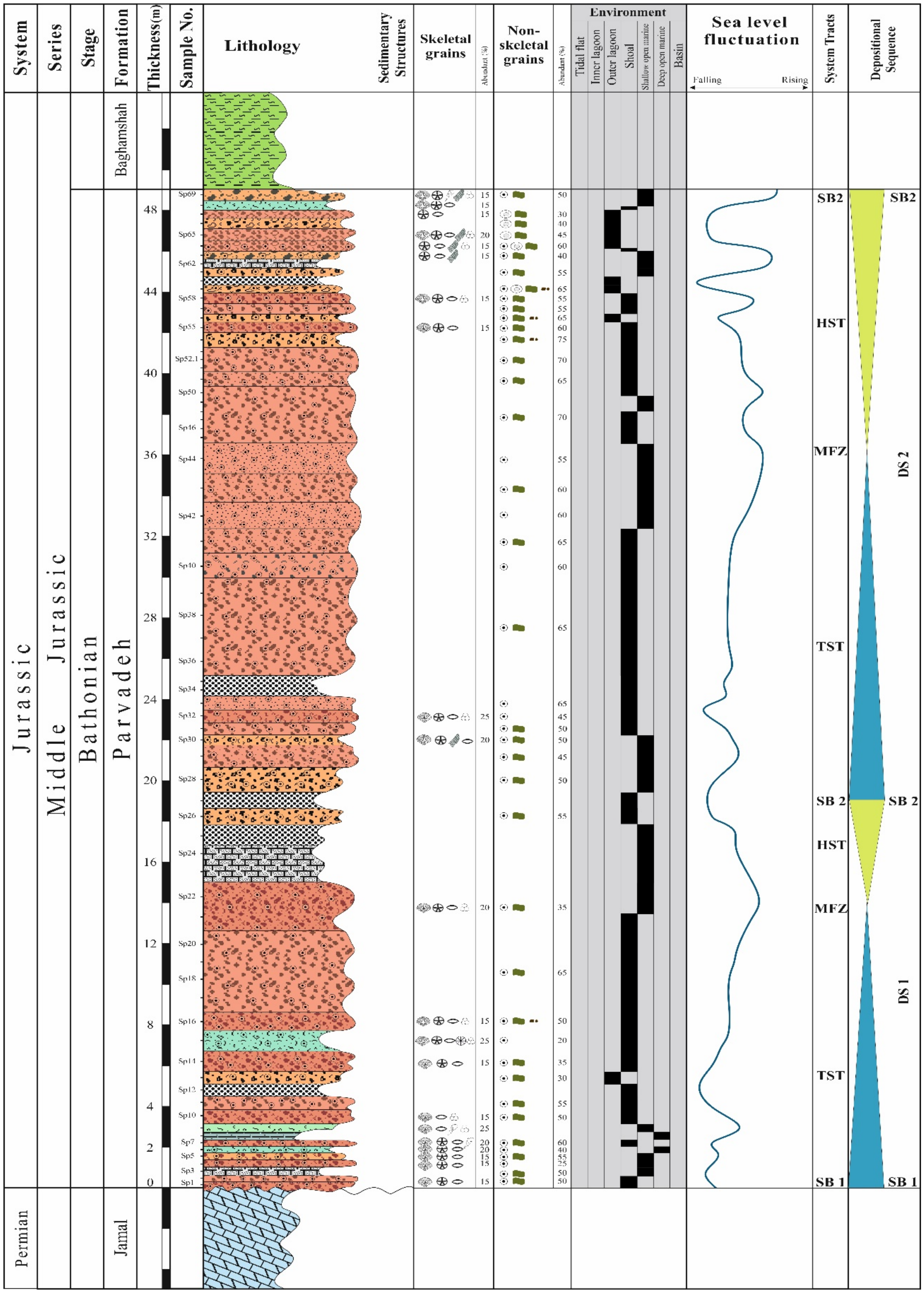

Figure 14. Sequence stratigraphy of Parvadeh Formation in Sikhuri section.

This sequence begins with LST which mostly consists of facies belonging to tidal flat and lagoon, and after that, by transgressive the sea level, TST has formed which mostly includes lagoon, shoal, and open marine facies. These facies include sandy intraclast pellet bioclast wackestone, bioclast wackestone/ packstone, sandy peloid wackestone/ packstone and sandy mudstone. Maximum flooding zone is mainly formed of open marine mudstone, wackestone and packstone facies. After TST, sea level has low fluctuations and HST is formed by deposition of sandy mudstone, bioclast pellet wackestone/ packstone and bioclast wackestone, which mainly belongs to open marine environment.

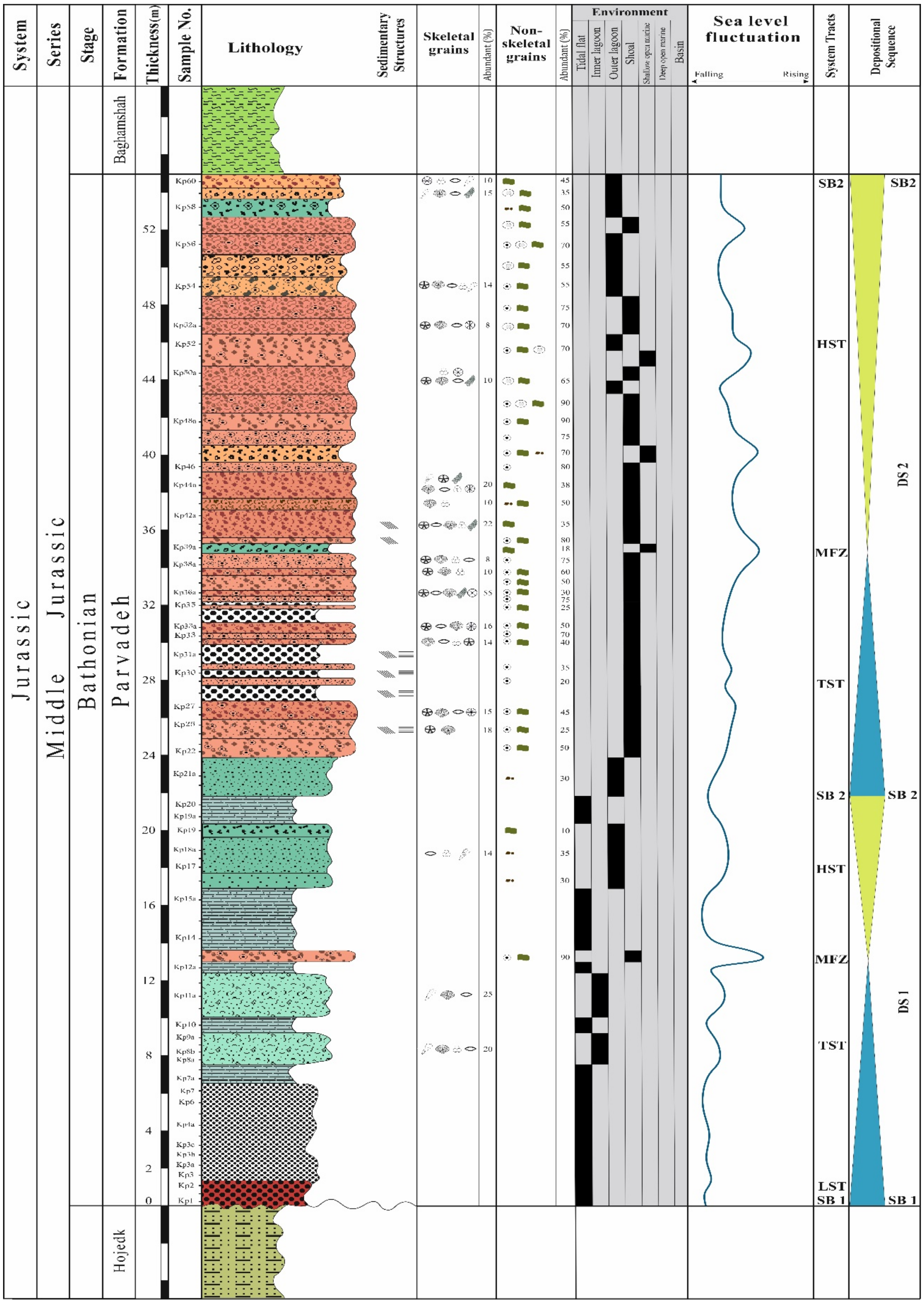

Figure 15. Sequence stratigraphy of Parvadeh Formation in Kalshaneh section.

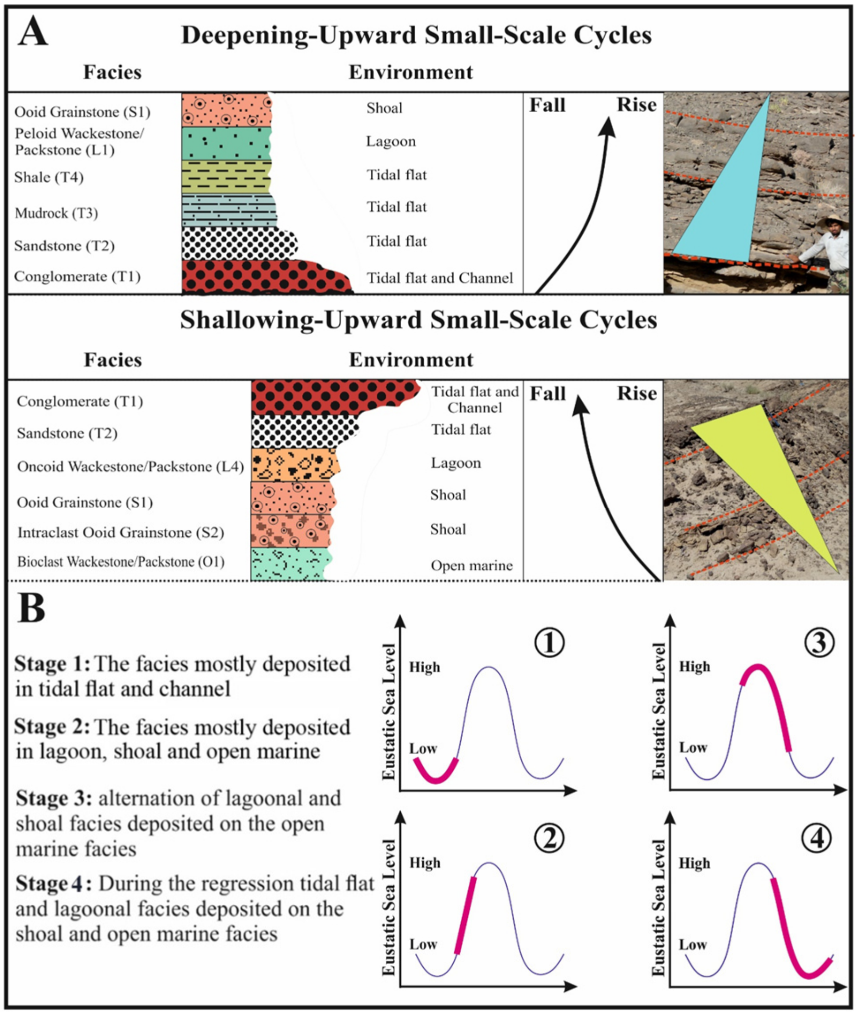

Figure 16. Small-scale shallowing and deepening cycles that mostly observed in the Parvadeh Formation successions (A) and different stages of sea level fluctuation that identified in depositional sequences based on Catuneanu, 2006 & Catuneanu *et al.,* 2009 (B).

In general, facies related to DS2 in South of Parvadeh section are formed in deeper environment suggesting that the basin is becoming deeper. After this depositional sequence, shale and marls of Baghamshah Formation continuously and non-erosionally have deposited on carbonated facies of Parvadeh Formation with second-typed sequence boundary (SB2) (Fig. 13). In Sikhuri section, sequence two (DS2) consists of TST and HST. This sequence begins with shoal and channel facies such as calcareous litharenite (calcarenite), intraclast ooid packstone/grainstone and continues with shoal and open marine facies including calcareous sandstone, intraclast ooid packstone, intraclast ooid grainstone (TST). Maximum flooding zone is related to deposits of shoal and open marine facies which composed of intraclast ooid packstone/ grainstone subfacies with bioclasts. After the maximum transgressive, small-scale fluctuations took place in the sea level and HST was formed with lagoon, shoal and open marine facies. In this sequence, facies properties mostly represent their formations in relatively high energy environments and appropriate conditions for open marine fauna (Fig. 14). In Kalshaneh section, DS2 begins with deposition of lagoonal facies and continues by transgression of sea level and deposition of shoal facies. Finally, Maximum flooding zone is specified by deposition of open marine intraclast wackestone subfacies containing pelecypod and brachiopoda fragments. HST in this sequence consists of semi-restricted lagoon and shoal facies which have been deposited due to sea level fluctuations. Boundary of this sequence with deposits of Baghamshah Formation is non-erosional SB2 sequence boundary and its thickness is about 33 meters (Fig. 15).

Sequences correlation and sea level fluctuation

The correlation of depositional sequences, surfaces and systems tracts is useful for better understanding the depositional history of mixed carbonate-siliciclastic complexes (Cateneanu *et al.,* 2011). In this study as discussed, in all depositional sequences, several small-scale shallowing and deepening upward cycles have been identified, including tidal flat, lagoon, shoal and open marine facies. In shallowing-upward cycles, usually tidal flat and lagoon facies deposited on shoal and open marine facies. But in deepening-upward cycles shoal and open marine facies deposited on lagoon and sometimes tidal flat facies. The general characteristics of the depositional sequences in the study sections are illustrated in Fig. 17.

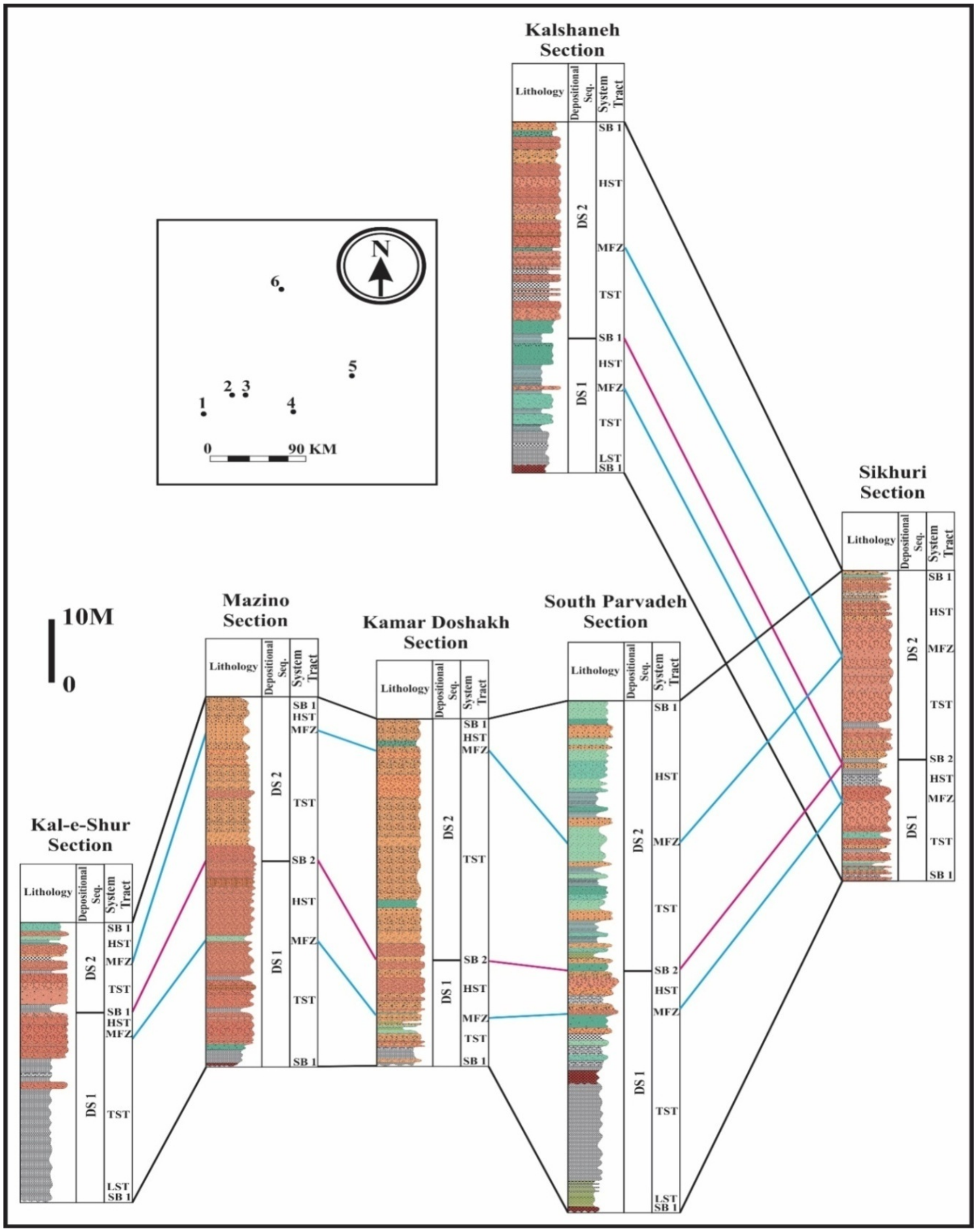

Figure 17. All of Sections, the boundary of DS2 with Baghamshah Fm is SB2, but in this figure, boundary was written SB1.

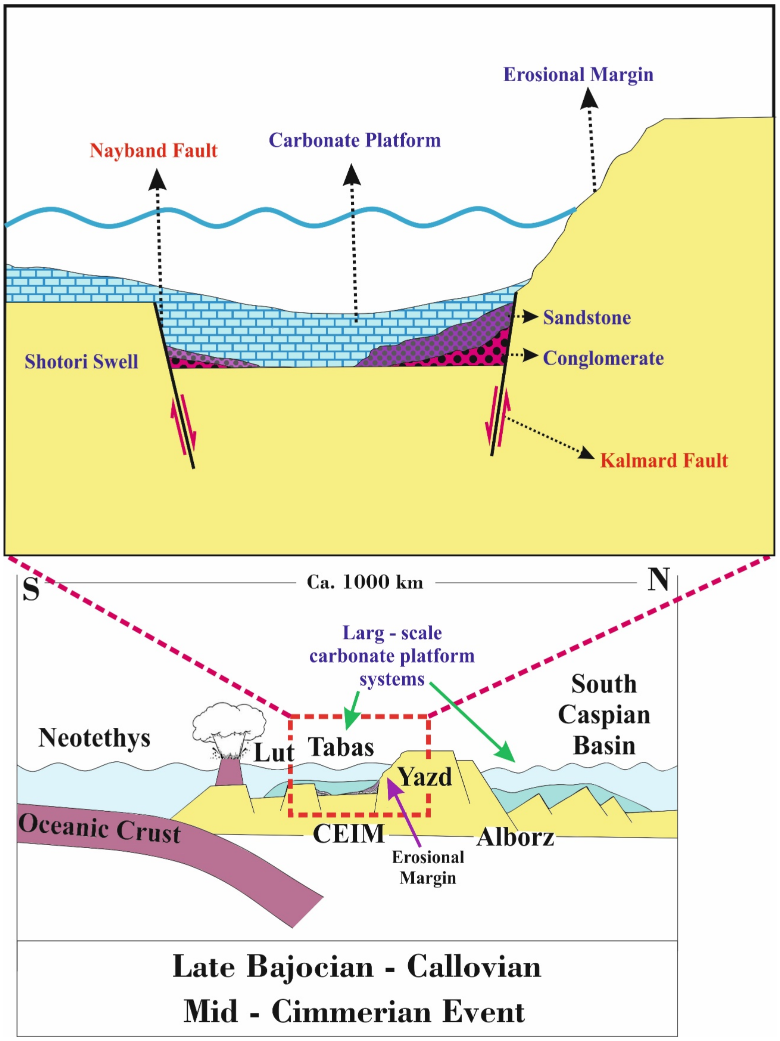

Figure 18. Paleogeographic and geodynamic model for the studied area in Tabas block at the time of Late Bajocian – Callovian (not to scale; CEIM, Central–East Iranian Microcontinent) (modified from Thierry, 2000; Wilmsen *et al.,* 2009b).

Interplay of various autocyclic or allocyclic mechanism such as tectonic, eustasy, subsidence, and sediment accumulation has been responsible for generating the high-frequency cycles. These small-scale cycles led to recognition of medium to large-scale cycles (Catuneanu *et al.,* 2009, 2011, 2013; Bai *et al.,* 2017). In Kal-e-Shur section, first sequence (DS1) is mainly formed of tidal flat and channel sandstones and at the end of sequence is mainly shoal and less amount of open marine facies (Fig. 17). In the second sequence (DS2), TST consists of shoal facies and HST is mostly lagoon facies. In Mazino section, facies are mostly related to shoal in sequence one (DS1) and in sequence two (DS2), they belong to lagoon environment. In Chah-e-Kamardoshakh section, in DS1 and DS2, most of facies belong to lagoon and somewhat shoal environments. In the south of Parvadeh section, DS1 is mostly formed of tidal flat sandstones and less amounts of lagoon facies at the end of sequence. At the time of DS2 formation in this section, sea level transgression has taken place and the open marine facies had been deposited. Sequences one and two in Sikhuri section mostly composed of shoal facies and less amount of lagoon and open marine facies. In Kalshaneh section, sequence one (DS1) is mostly composed of tidal flat and lagoon facies and sequence two is mostly formed of shoal facies and fewer amount of lagoon and open marine facies. Generally, according to the detail studies and the presence of facies in the studied sections, transgressive of sea level is observed from lower part to the upper part in the studied sections, which conforms to the sea transgression in a global scale (Haq *et al.,* 1987; Halam, 1988). Most facies in these sections belong to shallow marine environment from tidal flat to lagoon and open marine, of which tidal flat facies, lagoon and shoal have more frequency. Various factors can be effective in sea level changes in a region such as intra-basin and extra-basin factors like tectonic status, global changes in sea level and glaciers forming or melting (Husinec & Jelaska, 2006; Turner *et al.,* 2012; Catuneanu *et al.,* 2009, 2011, 2013, 2019; Bai *et al.,* 2017). Regarding the paleogeographic maps (Wilmsen *et al.,* 2009b; 2010) and also paleoclimate investigations, it can be mentioned that tectonic and global sea level changes more than other factors have affected the sea level changes in the studied area. The active tectonic status of the Tabas Block and the existence of important faults in this region, including the Kalmard, Nayband, Cheshme Rustam (a branch of the Nayband fault) faults, have had a relatively large impact on the deposition of siliciclastic and carbonate sediments in this area (wilmsen *et al.,* 2009b; Nazemi, 2013) (Fig. 18). The high thickness of detrital sediments in the Kalshaneh and Kalshour stratigraphic sections which are closer to the Yazd block and the Kalmard fault, indicate that these sediments have been originated from this block. The absence of siliciclastic sediments in the Sikhuri section can be attributed to the Shotori uplift relative to other Tabas subzones. In general, global sea level changes, Mid-Cimmerian tectonic events, Sediment supply, and local tectonic activities are important factors that have affected sedimentation of siliciclastic and carbonate deposits in the studied sections (e.g. Carpentier *et al.,* 2007; Badenas *et al.,* 2010; Bosence *et al.,* 2009).

Conclusion

Parvadeh Formation deposits (Bathonian), in the studied sections contained high variety of facies and formed in a marine carbonate ramp. These deposits contain skeletal and non-skeletal allochems which were formed in tidal flat, lagoon, shoal and open marine environment. Skeletal allochems show semi-restricted marine environment to open marine conditions. Variety in size of allochems, type of cements and their different textures show changes in the environments' energy level and depositional conditions during the formation of these depositional sequences. Presence of mixture siliciclastic (conglomerate and sandstone) and carbonate sediments and their sedimentary structures show the effect of waves and currents on the depositional environment. Detailed investigation of sedimentary facies and their integration with field and experimental observations led to identification of two third-order depositional sequences (DS1 and DS2). These facies are mostly abundant in transgressive systems tracts (TST) and highstand systems tracts (HST). Regarding these properties, sequence stratigraphy column and sea level fluctuations diagram in the study area have been drawn. Interplay of intra- and extra basin factors, such as tectonic, climate changes, local subsidence episodes and global sea level changes have been effective in these fluctuations during the Bathonian time.

References

Adabi, M.H., Salehi, M.A., Ghobeishavi, A., 2010. Depositional environment, sequence stratigraphy and geochemistry of Lower Cretaceous carbonates (Fahliyan Foemation), South–west Iran. Journal of Asian Earth Sciences 39, 148–160.

Adachi, N., Ezaki, Y., Liu, J., 2004. The origins of peloids immediately after the end–Permian extinction, Guizhou province, South China. Sedimentary Geology, 164: 161–178.

Adams, A., Diamond, L.W., 2019. Facies and depositional environments of the Upper Muschelkalk (Schinznach Formation, Middle Triassic) in northern Switzerland. Swiss journal of geosciences, 1–25.

Adnan, A., Shukla, U.K., Verma, A., Shukla, T., 2015. Lithofacies of transgressive–regressive sequence on a carbonate ramp in Vindhyan basin (Proterozoic): a case of tidal–flat origin from central India. Arabian Journal of Geoscience 8: 6985–7001.

Aghanabati, S.A., 1975. Etude geologique de la region de Kalmard (W. Tabas). Stratigraphie et tectonique. Geological Survey of Iran, Report 53: 239 pp.

Aghanabati, S.A., 1998. Jurassic Stratigraphy of Iran. Geological Survey of Iran.

Aghanabati, S.A., 2006. Geology of Iran, Geological Survey of Iran Publications, 586 pp.

Alavi, M., Vaziri, H., Seyed–Emami, K., Lasemi, Y., 1997. The Triassic and associated rocks of the Nakhlak and Aghdarband areas in central and northeastern Iran as remnants of the southern Turan active continental margin. Geological Society of America Bulletin, 109: 1563–1575.

Alsharhan, A.S., 2006. Sedimentological character and hydrocarbon parameters of the middle Permian to Early Triassic Khuff Formation, United Arab Emirates. GeoArabia, 11: 121–158.

Armenteros, I., Dabrio, C.J., Legoinha, P., González–Delgado, J.A., Martínez–Graña, A., Alonso–Gavilán, G., Civis, J., Pais, J., 2019. Facies and sequence analysis of Miocene open–shelf warm–temperate carbonates in Portimão (Lagos–Portimão Formation, Portugal). Facies, 65: 33.

Aurell, M., Robles, S., Badenas, B., Quesada, S., Rosales, I., Melendez, G., Garcia–Ramos, J.C., 2003. Transgressive/regressive cycles and Jurassic paleogeography of Northeast Iberia. Sedimentary Geology, 162: 239–271.

Bachmann, M., Hirsch, F., 2006. Lower Cretaceous carbonate platform of the eastern Levant (Galilee and the Golan Heights): stratigraphy and second–order sea–level change. Cretaceous Research, 27: 487–512.

Badenas, B., Aurell, M., 2010. Facies models of a shallow–water carbonate ramp based on distribution of non–skeletal grains (Kimmeridgian, Spain). Facies 56: 89–110.

Bai, H.Q., Betzler, C., Erbacher, J., Reolid, J., Zuo, F., 2017. Sequence stratigraphy of Upper Jurassic deposits in the North German Basin (Lower Saxony, Suntel Mountains). Facies, 63: 19.

Bayet–Goll, A., Shirezadeh Esfahani, F., Daraei, M., Monaco, P., Sharafi, M., Akbari Mohammadi, A., 2018. Cyclostratigraphy across a Mississippian carbonate ramp in the Esfahan–Sirjan Basin, Iran: implications for the amplitudes and frequencies of sea–level fluctuations along the southern margin of the Paleotethys. International Journal of Earth Science, 107: 2233–2263.

Berberian, M., King, G.C.P, 1981. Towards a paleogeographic and tectonic evolution of Iran. Canadian Journal of Earth Science, 18: 210–265.

Berbier, M., Hamon, Y., Callot, J.P., Floquet, M., Daniel, J.M., 2012. Sedimentary and diagenetic controls on the multiscale fracturing pattern of a carbonate reservoir: The Madison Formation (Sheep Mountain, Wyoming, USA). Marine and Petroleum Geology, 29: 50–67.

Berra, F., Felletti, F., Tessarollo, A., 2019. Oncoids and groundwater calcrete in a continental siliciclastic succession in a fault–controlled basin (Early Permian, Northern Italy). Facies, 65: 38.

Bjørlykke, K., 2010. Petroleum Geoscience: From Sedimentary Environments to Rock Physics. Springer–Verlag Berlin Heidelberg, 508 pp.

Bosence, D., Procter, E., Aurell, M., Bel Kahla, A., Boudagher–Fadel, M., Casaglia, F., Cirilli, S., Mehdie, M., Nieto, L., Rey, J., Scherreiks, R., 2009. A dominant tectonic signal in high–frequency, peritidal carbonate cycles? A regional analysis of Liassic platforms from Western Tethys. Journal of Sedimentary Research, 79: 389–415.

Boulin, J., 1988. Hercynian and Eocimmerian events in Afghanistan and adjoining regions. Tectonophysics, 148: 253–278.

Bover–Arnal, T., Salas, R., Moreno–Bedmar, J.A., Bitzer, K., 2009. Sequence stratigraphy and architecture of a late Early–Middle Aptian carbonate platform succession from the western Maestrat Basin (Iberian Chain, Spain). Sedimentary Geology, 219: 280–301.

Brachert, T.C., Hultzsch, N., Knoerich, A.C., Krautworst, U.M.R., Stuchkrad, O.M., 2001. Climatic signatures in shallow–water carbonates: high–resolution stratigraphic markers in structurally controlled carbonate buildups (Late Miocene, southern Spain). Paleogeography Paleoclimatology Paleoecology, 175: 211–237.

Burchette, T.P., Wright, V.P., 1992. Carbonate ramp depositional systems. Journal of Sedimentary Geology, 79: 3–35.

Burchette, T.P., Wright, V.P., Faulkner, T.J., 1990. Oolithic sand body depositional models and geometries, Mississippian of southwest Britain: implication in carbonate ramp settings. Sedimentary Geology, 68: 87–115.

Cadjenovic, D., Kilibarda, Z., Radulovic, N., 2008. Triassic to Late Jurassic evolution of the Adriatic carbonate platform and Budva Basin, Southern Montenegra. Sedimentary Geology, 24: 1–17.

Carozzi, A., 1989. Carbonate rocks depositional model. Prentice Hall, NewJersy, 604 pp.

Carozzi, A., 1993. Sedimentary petrology. Englewood Cliffs (NJ), Prentice Hall, 263 pp.

Carpentier, C., Lathuilière, B., Ferry, S., Sausse, J., 2007. Sequence stratigraphy and tectonosedimentary history of the Upper Jurassic of the Eastern Paris Basin (Lower and Middle Oxfordian, northeastern France). Sedimentary Geology, 197: 235–266.

Catuneanu, O., 2006. Principles of sequence stratigraphy. Amsterdam, Elsevier, 375 pp.

Catuneanu, O., 2019. Model–independent sequence stratigraphy, Earth Science Reviews, 188: 312–388.

Catuneanu, O., Abreu, V., Bhattacharya, J.P., Blum, M.D., Dalrymple, R.W., Eriksson, P.G., Fielding, C.R., Fisher, W.L., Galloway, W.E., Gibling, M.R., 2009. Towards the standardization of sequence stratigraphy. Earth Science Review, 92: 1–33.

Catuneanu, O., Galloway, W.E., Kendall, C.G.S.t.C., Miall, A.D., Posamentier, H.W., Strasser, A., Tucker, M.E., 2011. Sequence stratigraphy: methodology and nomenclature. Newsletters Stratigraphy, 44: 173–245.

Catuneanu, O., Zecchin, M., 2013. High–resolution sequence stratigraphy of clastic shelves II: controls on sequence development. Marine and Petroleum Geology, 39: 26–38.

Cluff, R.M., 1984. Carbonate sand shoals in the middle Mississippian (Valmeyeran) Salem–St. Louis–Ste. Genevieve Limestones, Illinois Basin, in P.M. Harris, ed., Carbonate Sands – A Core Workshop. SEPM Core Workshop 5, 94–135.

Corda, L., Brandano, M., 2003. Aphotic zone carbonate production on a Miocene ramp, Central Apennines, Italy. Sedimentary Geology, 161: 55–70.
Dunham, R.J., 1962. Classification of carbonate rocks according to depositional texture. American Association of Petroleum Geology, Memoir, 1: 108–121.
Ehrenberg, S.N., Pickard, N.A.H., Svana, T.A., Oxtoby, N.H., 2002. Cement geochemistry of photozoan carbonate strata (Upper Carboniferous–Lower Permian), Finnmark carbonate platform, Brents Sea. Journal of Sedimentary Research, 72: 95–115.
Elgadi, M.S.M., Brookfield, M.E., 1999. Open carbonate ramp facies, microfacies and paleoenvironments of the Gramame Formation (Maastrichtian), Pernambuco–Paraibba Basin, Northeastern Brazil. Journal of South American Earth Sciences, 12: 411–433.
Embry, A.F., 2002. Transgressive–regressive (TR) sequence stratigraphy. Sequence Stratigraphic Models for Exploration and Production: Evolving Methodology, Emerging Models and Application Histories, 22:151–172.
Embry, A.F., Klovan, J.E., 1972. Absolute water depth limits of late Devonian paleoecological zones. Geologische Rundschau 61: 672–686.
Farry, J.L., Van Hassel, J.H., 2007. Freshwater Bivalve Ecotoxicology. Society of Environmental Toxicology and Chemistry, 375 pp.
Flügel, E., 2010. Microfacies of Carbonate Rocks, analysis interpretation and application, Berlin, Heidlberg, New York. Springer–Verlag, Berlin, 976 pp.
Folk, R.L., 1980. Petrology of Sedimentary Rocks. Hemphill Publishing Co, Austin, Texas, 182 pp.
Fürsich, F.T, Wilmsen, M., Seyed–Emami, K., Majidifard, M.R, 2003. Evidence of synsedimentary tectonics in the Northern Tabas Block, east–central Iran: The Callovian (Middle Jurassic) Sikhor Formation. Facies, 48: 151–170.
Geel, T., 2000. Recognition of stratigraphic sequences in carbonate platform and slope deposits: empirical models based on microfacies analysis of Palaeogene deposits in southeastern Spain. Palaeogeography, Palaeoclimatology, Palaeoecology, 155: 211–238.
Halam, A., 1988. A reevaluation of jurassic Eustasy in the light of new data and the revised exxon curve. In: Wilgus, C.K., Hastings, B.S., Posamentire, E., Vanvagoner, J., Ross, C.A., Kendall, C.G. (Eds.), Sea Level Changes: an Integrated approach, Society of Economic Paleontologists and Mineralogists. Special Publication, 42: 3–39.
Hallock, P., Glenn, E.C., 1986. Larger foraminifera: A Tool for Paleoenvironmental analysis of Cenozoic carbonate depositional facies. Palaios, 1: 55–64.
Haq, B.U., 1991. Sequence stratigraphy, sea level change and significance for the deep sea, In Macdonald, D.I.M edition. Journal of sedimentation and tectonics, 12: 3–39.
Haq, B.U., Hardenbol, J., Vail, P.R., 1987. Chronology of fluctuating sea levels since the Triassic. Science, 235: 1156–1167.
Hueneke, H., Mulder, T., 2011. Deep Sea Sediments. Elsevier, 849 pp.
Husinec, V., Jelaska, A., 2006. Relative sea–level changes recorded on an isolated carbonate platform: Titonian to Cenomanian succession, Southern Croatia Journal of Sedimentary Research, 76: 1120–1136.
Javidan, M., Mokhtarpour, H., Sahraeyan, M., Kheyrandish, H., 2015. Lithofacies, architectural elements and tectonic provenance of the siliciclastic rocks of the Lower Permian Dorud Formation in the Alborz Mountain Range, Northern Iran. Journal of African Earth Sciences, 109: 211–223.
Ketzer, J.M.M., 2002. Diagenesis and Sequence Stratigraphy, Comprehensive Summaries of Uppsala. Dissertations from the Faculty of Science and technology 762, University of Uppsala, Uppsala, 30 pp.
Khalifa, M.A., Catuneanu, O., 2008. Sedimentology of the fluvial and fluvio–marine facies of the Bahariya formation (Early Cenomanian), Bahariya Oasis, western Desert, Egypt. Journal of African Earth Sciences, 51: 89–103.
Koehrer, B., Heymann, C., Prousa, F., Aigner, T., 2010. Multiple–scale facies and reservoir quality variations within a dolomite body – Outcrop analog study from the Middle Triassic, SW German Basin. Marine and Petroleum Geology, 27: 386–411.
Maurer, F., Martini, R., Rettori, R., Hillgärtner, H., Cirilli, S., 2009. The geology of Khuff outcrop analogues in the Musandam Peninsula, United Arab Emirates and Oman.GeoArabia, 14: 125–158.
Mehdizadeh, M., 2010. Litho–biostratigraphy of Parvadeh Formation in Tabas Area with special attitude to Ammonite biological zones of this Formation. MSc Thesis, Tehran Azad University (Science and Research Branch), 161 pp.
Miall, A.D., 2014. Fluvial Depositional Systems. Springer, 315 pp.
Nazemi, M., 2013. Symptoms of earthquake active folding in the east and southeast of Tabas. PhD thesis, Islamic Azad University Science and Research Branch, 122 pp.
Pandey, D. K., Fürsich, F.T., 2003. Jurasic corals from east–central Iran. Beringeria, 140 pp.
Patra, A., Singh, B.P., 2015. Facies characteristics and depositional environments of the Paleocene–Eocene strata of the Jaisalmer basin, western India. Carbonates Evaporites, 30: 33–346.
Pleş, G., Oprişa, A., Bucur, I.I., Săsăran, E., Mircescu, C.V., Oltean, G., Iacob, R.G., 2019. The central–western Getic

Carbonate Platform: Upper Jurassic to Lower Cretaceous biostratigraphy and sedimentary evolution of the Cioclovina–Băniţa sector (Southern Carpathians, Romania). Facies 65: 32.

Pomar, L., 2001. Types of carbonate platforms: a genetic approach. Basin Research, 13: 313–334.

Rahmani, M., 2014a. Lithostratigraphy, lithofacies, sedimentary environment and coral fauna of Parvadeh Formation located in Tabas area, east–central of Iran. MSc thesis, Kerman Institute of Higher Education, 105 pp.

Rahmani, M., Dastanpour, M., Khanebad, M., Yahya–Sheibani, V., Zaman, S., 2014c. Stratigraphy and Paleontology of the Coral Parvadeh Formation in the Mazino Coal Mines Area, Tabas Block, First National Iranian Conference of Sedimentology, Isfahan, Iran.

Rahmani, M., Khanebad, M., Dastanpour, M., Yahya–Sheibani, V., 2014b. Facies and sedimentary environment of Parvadeh Formation in Kalashaneh section in the north of Tabas, first national Iranian conference of sedimentology, Isfahan, Iran.

Sabbagh Bajestani, M., Mahboubi, A., Moussavi–Harami, R., Al–Aasm, I., Nadiafi, M., 2017. Facies analysis and sequence stratigraphy of the Qal,eh Dokhtar Formation (Middle–Upper Jurassic) in the West of Boshrouyeh, East central Iran. Acta Geologica Sinica–English Edition, 91: 1797–1819.

Saidi, A., Brunet, M.F., Ricou, L.E. 1997. Continental accretion of the Iran Block to Eurasia as seen from Late Paleozoic to Early Cretaceous subsidence curves. Geodinamica Acta, 10: 189–208.

Salehi, M. A., Moussavi–Harami, R., Mahboubi, A., Fürsich, F.T., Wilmsen, M., Heubeck, C., 2017. A tectono–stratigraphic record of an extensional basin: the Lower Jurassic Ab–Haji Formation of east–central Iran. Swiss Journal of Geoscience.

Schlager, W., 2003. Benthic carbonate factories of the Phanerozoic. International Journal of Earth Science, 92: 445–464.

Seyed–Emami, K., Fürsich, F.T., Wilmsen, M., 2004. Documentation and significance of tectonic events in the Northern Tabas block (east–central Iran) during the Middle and Late Jurassic. Rivista Italiana di Paleontologia e Stratigrafia, 110: 163–171.

Seyed–Emami, K., Fursich, F.T., Wilmsen, M., 2006. New evidence on the lithostratigraphy of the Jurassic System in the northern Tabas Block, east–central Iran. Geosciences, 15: 75–97.

Seyed–Emami, K., Schairer, G., Fürsich, F.T., Wilmsen, M., Majidifard, M.R., 2000. First record of ammonites from the Badamu formation at the Shotori Mountains (central Iran). Eclogae Geologicae Helvetiae, 93: 257–263.

Sim, C.I.P., Onuoha, K.M., Okwara, I.C., Okonkwo, I.A., Ibemesi, P.O., Facies analysis and depositional environment of the Campano – Maastrichtian coal–bearing Mamu Formation in the Anambra Basin, Nigeria, Journal of African Earth Sciences. (2019), doi: 10.1016/j.jafrearsci.01.011.

Sinclair, H.D., Sayer, Z.R., Tucker, M.E., 1998. Carbonate sedimentation during early foreland basin subsidence: The Eocene succession of the French ALPS. In: Wright V.P., Burchette T.P. (eds), Carbonate ramps. Special Publication Geological Society of London, 149: 205–227.

Stampfli, G.M., Borel, G.D., 2002. A plate tectonic model for the Paleozoic and Mesozoic constrained by dynamic plate boundaries and restored synthetic oceanic isochrones. Earth and Planetary Science Letters 196, 17–33.

Stocklin, J., 1968. Structural history and tectonics of Iran; a review. American Association of Petroleum Geologists Bulletin, 52: 1229–1258.

Tamura, T., Masuda, F., 2003. Shallow–marine fan delta slope deposites with large–scale cross–stratification: the Plio–Pleistocene Zaimokuzawa Formation in th Ishikari Hills, northern Japan. Sedimentary Geology 158: 195–207.

Tcherepanov, E.N., Droxler, A.W., Lapointe, P., Mohn, K., 2008. Carbonate seismic stratigraphy of the Gulf of Papua mixed depositional system: Neogene stratigraphic signature and eustatic control. Basin Research, 20: 185–209.

Thierry, J., 2000. Middle Callovian (157–155 Ma). In: Dercourt, J., Gaetani, M. *et al.,* (eds) Atlas Peri–Tethys Palaeogeographical Maps, CCGM/CGMW, Paris, 71–97.

Tucker, M.E., 2003. Sedimentary Rocks in the Field, 3rd edition.

Turner, B.R., Armstrong, H.A., Wilson, C.R., Makhlouf, I.M., 2012. High frequency eustatic sea–level changes during the Middle to early Late Ordovician of southern Jordan: Indirect evidence for a Darriwilian Ice Age in Gondwana. Sedimentary Geology, 251: 34–48.

Valipour Goodarzi, B., Khazaei, A., Zamani, S., Mirab Shabestari, G., 2015. Paleontological study of the Parvadeh Formation based on Sclerctina corals (middle Jurassic) in the southwest of Tabas. Journal of Sedimentary Facies, 8: 302–290.

Van Wagoner, J.C., Mitchum, R.M., Campion, K.M., Rahmanian. V.D., 1990. Siliciclastic sequence stratigraphy in well logs, cores, and outcrops. American Association of Petroleum Geologists Bulletin, Methods Explor 7: 55.

Van Wagoner, J.C., Posamentier, H.W., Mitchum, R.M., Vail, P.R., Sarg, J.F., Loutit, T. S. Hardenbol, J., 1988. An Overview of the Fundamentals of Sequence Stratigraphy and Key Definitions. In: Wilgus, C.K., Ross, C.A., Kendall, C.G.St.C., Posamentier, H. W., Van Wagoner, J.C., (eds): Sea–Level Changes: An Integrated Approach. SEPM Special Publication, 42: 39–45.

Wilmsen, M., Fürsich, F., Seyed–Emami, K., Majidifard, M., Zamani–Pedram, M., 2010. Facies analysis of a large–scale

Jurassic shelf–lagoon: the Kamar–e–Mehdi Formation of east–central Iran. Facies, 56: 59–87.
Wilmsen, M., Fürsich, F.T., Seyed–Emami, K., 2003. Revised lithostratigraphy of the Middle and Upper Jurassic Magu Group of the northern Tabas Block, east–central Iran. Newsletters on Stratigraphy, 39: 143–156.
Wilmsen, M., Fürsich, F.T., Seyed–Emami, K., Majidifard, M.R., 2009a. An overview of the stratigraphy and facies development of the Jurassic System on the Tabas Block, east–central Iran. Geological Society of London, Special Publications, 312: 323–343.
Wilmsen, M., Fürsich, F.T., Seyed–Emami, K., Majidifard, M.R., Taheri, J., 2009b. The Cimmerian Orogeny in northern Iran: tectono–stratigraphic evidence from the foreland. Terra Nova 21: 211–218.
Wilmsen, M., Wiese, F., Seyed–Emami, K., Fürsich, F.T., 2005. First record and significance of Turonian ammonites from the Shotori Mountains, east–central Iran. Cretaceous Research, 26: 181–195.
Wilson, J.L., 1975. Carbonate facies in geologic history. Berlin, Springer.
Yilmaz, I.O., Altiner, D., 2007. Cyclostratigraphy and sequence boundaries of inner platform mixed carbonate–siliciclastic successions (Barremian–Aptian) (Zonguldak, NW Turkey). Journal of Asian Earth Sciences 30: 253–270.
Zamani–Pedram, M., 2011. Source, facies, and sedimentary environments of the Middle to Upper Jurassic strata in the Kerman and Tabas areas, east–central Iran. PhD thesis, Julius–Maximilians–Universität Würzburg, 212 pp,
Zarrin, M., Mirab Shabestari, G., Khazaei, A., 2016. Sedimentary environment, diagenesis and geochemistry of the Parvadeh Formation (Middle Jurassic) in the Kamar–Mahdi section (southwest of Tabas). Journal of Sedimentary Facies 9: 121–145.